# DETECTION AND DELINEATION OF CONTAMINANT MIGRATION USING THE TERRAIN CONDUCTIVITY TECHNIQUE OUTSIDE THE PERIMETERS OF THE DOMPOASE LANDFILL FACILITY IN KUMASI – GHANA



**By**

**Elvis Boateng**

**B.Sc. Physics (Hons)**

**A Thesis submitted to the Department of Physics, Kwame Nkrumah University of Science and Technology in partial fulfilment of the requirements for the degree**

**of**

**MASTERS OF SCIENCE**

**(Geophysics)**

**College of Science**

**JULY 2012**

**DECLARATION**

I hereby declare that this submission is my own work towards the MSc and that, to the best of my knowledge, it contains no material previously published by another person nor material which has been accepted for the award of any other degree of the University, except where due acknowledgement has been made in the text.

ELVIS BOATENG PG20064157 .................... .................... 21/03/2013 ....................

Student Name & ID Signature Date

Certified by

VAN-DYCKE ASARE .................... .................... 25/3/2013 ....................

Supervisor(s) Name Signature Date

Certified by

Prof. S.K. Donkor .................... .................... 25/3/13 ....................

Head of Dept. Name Signature Date

# ABSTRACT

Electromagnetic conductivity survey has been performed outside the perimeters of an active municipal landfill facility in Dompoase, a suburb of Kumasi in the Ashanti Region of Ghana. The study was undertaken to identify potential conductive layers probably connected with leachate communicationfrom the landfill.The Geonics EM 34-3 terrain conductivity equipment was employed as the geophysical tool for the EM survey. Operating in the low induction number regime, three intercoil separations of 10, 20 and 40 m were used in both the horizontal and vertical dipole configurations. The specific area of interest was the two sides of a discharge stream which carries water from the treatment ponds. The data was acquired along sixteen east – west profiles, each of length 100 m, running approximately perpendicular to the discharge stream. There were seven and nine profiles respectively on the right and left sides of the discharge stream. The total area covered is approximately 1400 $m^2$. The distance between measurement points was 10 m.The high conductivity found within the depths 30 to 60 m close to thesouthern boundary of the landfill might suggest leachate communication from the landfill. The linear pattern of the contour lines in that anomalous zone probably indicate the presence of zones of weakness trending approximately perpendicular to the direction of flow of the discharge stream. This weak zone could account for the lateral spread of leachate within those depths, where leachate plume has so far migrated about 30 m from the ~~landfill~~ southern boundary.A major implication of these conclusions is in terms of aquifer protection. In terms of aquifer protection it must be noted that the aquifer in the adjoining land is considerably well protected. The overburden in major part of the surveyed area is quite thick.

## DEDICATION

This thesis is dedicated to all members of my family especially my mother Peace MawuseAmedorme and AmaDufieFosu for their support and prayer towards a successful completion of this work.

## ACKNOWLEDGMENTS

The successful completion of this work came about as result of a massive contributions made by several people; without whom the work would not have materialised. I therefore, deem it necessary to express my profound gratitude to all such people.

I first express my profound gratitude to my dynamic and hardworking supervisor, Mr Van-DyckeAsare who encouraged, supervised and guided me through.My thanks also go to Abuenyi Bernard, a brother and a friend, who in diverse ways contributed to the successful completion of this work.

I will also like to extend special thanks to the workers and operators of the Dompoase Sanitary Landfill and Septic Treatment Facility for allowing access to their facility and for providing background on the development and operations.

To all others whose names cannot be readily mentioned, I am equally grateful to them.

**CONTENTS**

# CHAPTER ONE

# GENERAL INTRODUCTION

## 1.1 Background

Groundwater is water that exists within soils and fractured rocks underneath the ground. Groundwater is usually replenished by rain water. The process whereby rain water seeps into the ground is called infiltration. The soils and rocks that holds the water underneath the ground is called an aquifer. When groundwater is being replenished, the aquifer usually gets saturated with water. The top of this saturated zone is called the water table. By reason of its location, groundwater is often cleaner than surface water. Groundwater is usually protected against contamination from the surface by soils and covering rock layers. This is why most drinking water in many areas of the world is groundwater. For example, research indicates that up to 80% of drinking water in Europe, Russia and Africa is from groundwater (Wihelm et al, 2005). However, rising world population, changes in land use and rapid industrialization increasingly place soil and groundwater at risk of contamination. Contamination of the subsurface can take place in many ways: pollution of groundwater or soil through direct contamination, saltwater intrusion, or leakage from buried waste, landfill or even a cemetery (Bastianon et al., 2000).

Land use such as landfilling, which produces leachate has been found to be one of the major sources of contamination of groundwater (Bjerg et al, 2003), Chofqi et al. 2004; and Christensen et al. 1994; have reported the contamination of ground water by landfill leachate. Contamination of groundwater by landfill leachate may even eventually lead to surface water contamination because groundwater usually discharges to surface water bodies such as lakes and rivers (Freeze & Cherry 1979). Non-organic (ionic) groundwater contamination from leachate usually results in an increase in the conductivity of the groundwater. For example, in a sandy soil, the addition of 25 ppm of ionic material to groundwater increases ground conductivity by approximately 1 mS/m.

To contain the above potential hazards, Sanitary Engineered Landfills are employed as alternative means of disposing and managing municipal solid waste. Sanitary Engineered Landfills have highly engineered containment systems designed to minimize the impact of solid waste disposal on the environment and ultimately on human health (Kerry et al, 2005). However, sanitary landfills may not be without flaws; the containment systems may not absolutely prevent leaching and could also suffer from some form of structural failure which may not readily be detected. For these and other reasons, engineered landfills have groundwater monitoring wells to assess the state of groundwater in the area from time to time.

These monitoring wells are sometimes not enough or spread widely around the periphery of the facility and within the contiguous lands to assess the impact of the landfill leachate on the surrounding groundwater. For the same reasons as stated above, the sampling wells may not be able to indicate the lateral and vertical spread of contaminants and finally the cost involved in conducting laboratory analyses may be prohibitive and may prevent landfill operators from conducting regular and periodic groundwater assessment.

Electromagnetic (EM) methods utilizing controlled sources have traditionally been used in near-surface geophysical investigations such as mineral and hydrocarbon exploration as well as in geological mapping and structural studies. Recently, the EM methods have become popular in environmental and engineering investigations (Markku, 2003). The method offers a non-invasive and cost effective tool for identifying subsurface contamination and delineating the lateral extent of contaminant intrusion into the groundwater system. The EMI's sensitivity to soluble salts makes it an effective tool for the assessment of surface and groundwater contamination from animal wastes and landfill site (Bowling et al., 1997).



Electromagnetic surveys have been used for landfill boundary detection (Mack and Maus, 1986; McQuown et al., 1991; Scaife, 1990; Stenson, 1988) and detection of leachate contaminant plumes (Hall and Pasicznyk, 1987; Mack and Maus, 1986; Russell, 1990; Walther et al., 1986). Several researchers have also been successful in using EM surveys to identify volatile organic plumes such as gasoline (Fawcett, 1989; Olhoeft, 1986; Olhoeft and King, 1991; Saunders and Cox, 1987).

The current study aims at conducting Electromagnetic Induction Terrain Conductivity measurements using the EM34-3 to assess the potential effect of contaminants on the groundwater around the perimeter of one of the major engineered sanitary landfill facilities in Kumasi, Ghana.

## 1.2 Problem Statement

The Kumasi Sanitary Landfill and Septic waste treatment facility commissioned six years ago covers an overall area of 40 hectares. The site admits industrial waste, domestic waste, and septic waste for treatment. The challenge, however, is that the site has only two wells for groundwater monitoring, which is inadequate and cannot completely characterize the state of the underground water. In addition to this, interactions with site operators revealed that there has not been any groundwater investigation since the facility become operational six years ago.



Reconnaissance at the facility and interaction with the facility supervisors revealed that high volumes of leachate are generated daily. The landfill has a network of pipes and trenches to collect these leachates for treatment. Though the facility has not caused any environmental problems, particularly from the leachate seeping out of the refuse pile into the adjoining groundwater system, the high volumes of waste admitted daily and the seasonal heavy downpour makes it imperative to study leachate communication from the landfill to the adjoining region. Any potential contamination, if not addressed will put the life of those neighbouring residents who depend on groundwater in danger of contracting diseases such as cholera and typhoid. The problem is to detect and map the extent of possible contamination of the contiguous lands by leachate from the landfill facility, in the presence of conductivity variations caused by other parameters such as changing lithology, by using the electromagnetic induction survey.

### 1.3 Objectives of the study

The main aim of the study is to use Electromagnetic Induction Survey Method to ascertain if, and to what extent, the groundwater in the contiguous lands of the Kumasi landfill and septic treatment facility is contaminated.

Specifically, the research aims at achieving the following objectives:

1. To study the geology of the area by identification of the soil types in the laboratory and from literature.
2. To determine the direction of ground water flow in other to predict areas around the landfill site that is likely to be affected if there is ground water contamination or pollution.
3. To map the lateral conductivity variations in the lands coterminous to landfill facility.
4. To determine whether leachate plumes are migrating away from the landfill and from the discharge stream towards the fallow contiguous lands
5. To obtain information about the variation of conductivity with depth in order to estimate the thickness and bulk conductivity of the overburden.
6. To make recommendations on areas around the landfill where monitoring wells should be sited to monitor groundwater quality.

### 1.4 Justification of objectives

Leachates have been implicated in many environmental pollution, surface and groundwater pollution worldwide. Drinking contaminated groundwater can have serious health effects. Diseases such as hepatitis and dysentery may be caused by contamination from septic tank waste. Poisoning may be caused by toxins that have leached into well water supplies. Wildlife can also be harmed by contaminated groundwater. Other long term effects such as certain types of cancer may also result from exposure to polluted water. It is therefore imperative to evaluate the potential of groundwater contamination as a result of leachate migration so that the necessary remedial measures could be taken to avert any health and environmental crisis.

A fair idea of the geology of the host area can help determine the types of rocks, their porosity and degree of fracture so that a prediction can be made of the direction of possible leachate migration. The determination of direction of groundwater flow will help determine the regions around the landfill where the investigations would be carried out. It will also help predict the direction where leachate will flow if it gets in contact of the surrounding groundwater.

The traditional way of monitoring groundwater using wells has been found to be expensive, scarce and commonly fail to define the full extent of contamination (Peter et al, 2002). In this respect, geophysical Electromagnetic Induction (EMI) survey methods have emerged as useful tools to characterize both horizontal and vertical extent of groundwater contamination. The geophysical method offers innovative and noninvasive tool for identifying subsurface contamination in these situations. Electromagnetic induction has been used by researchers to infer the relative concentration, extent, and movement of animal waste products in soils, because of its sensitivity to soluble salts (Bowling et al., 1997; Brune and Doolittle, 1990; Drommerhausen et al., 1995; Eigenberg and Nienaber, 1998; Eigenberg et al., 1998; Radcliffe et al., 1994; Ranjan and Karthigesu, 1995; Siegrist and Hargett, 1989; Stierman and Ruedisili, 1988).

This research, apart from identifying the potential contamination of groundwater is also to find out how effective EMI method can be used in investigating groundwater contamination and to recommend it to authorities managing the facility.

## 1.5 Scope of the Study

### 1.5.1 Geology and Terrain Evaluation

The geology and topographical study of the area would be undertaken by site tour, observations of soil type and rock outcrops. Surface water direction would be determined to infer possible ground water direction and gradient of the site. This would help select a suitable region around the site where the investigation would be carried out

### 1.5.2 Geophysical Measurements

In this investigation apparent ground conductivity will be measured using Geonics EM34-3 instrument. The EM34-3 is a two-man portable instrument which has two coils flexibly connected. The intercoil spacing is measured electronically so that the receiver operator simply reads a meter to accurately set the coils to the correct spacing which can be 10, 20 or 40 meters so as to directly vary the effective depth of exploration form 7.5 m to about 60 m.

The survey region will be divided into 10 profile lines with each profile line 10 m apart. On each profile line 10 observation points, 10 m apart will be marked. At each observation point the horizontal dipole (HD) mode reading would be taken first, followed by the vertical dipole (VD) mode, to probe different depths based on the respective intercoil spacing (10 m, 20 m and 40 m).

For the HD mode the receiver ($R_x$) and transmitter ($T_x$) coils would be placed on the ground in such a way that their axes are parallel, but their planes would be coplanar and vertical to the ground surface. The instrument receiver coil would then be moved back and forth until the meter indicated a null setting and the terrain conductivity read from a second digital meter and recorded. Similarly, for the VD mode the coils would be placed on the ground with their axes parallel, and coplanar. The procedures at each station would be repeated until the desired total length of each traverse line is covered. The measurements would be recorded in millisimens per meter ($mSm^{-1}$).



The recorded field data would be contoured using gridding, contouring and surface mapping software, Surfer 10. The data will also be used to generate a two layered model of the subsurface using an EM34 Modeling program called FreqEM ver 1.00. Contouring the data has some specific advantages. Firstly it gives clear overall terrain conductivity over the entire survey area in each mode of operation (i.e. HD & VD) and intercoil spacing which is more convenient than profile by profile.

### 1.6 Organisation of the Thesis

This work consists basically of six chapters. Subsequent to this introduction, the second chapter gives an overview of the soil profile, soil moisture and groundwater. The discussions in this chapter extend to groundwater contamination, landfill and leachate generation from landfills. It also reviews some geophysical methods used to attack such environmental problems. Thereafter, the third chapter deals with the theory of the electromagnetic induction survey method, the location and description of the study site, the layout of the profiles and finally the geophysical data acquisition. In chapter four, the main results are presented and briefly described. In chapter five the results are discussed. As a conclusion to this work, chapter six again summarizes the obtained results of the preceding chapter in the context of the aims and objectives of the whole work.

## CHAPTER TWO

## THE SOIL, SOIL CONTAMINATION BY LEACHATE AND REVIEW OF GEOPHYSICAL METHODS OF DETECTION

### 2.1 Soil Constituent

Soils consist basically of four components namely minerals, organic matter, water and gases

**Mineral materials:** Soil minerals are usually made up of clay, silt and sand. The minerals are formed from weathered parent rocks such as granite. Soils are classified on the basis of texture or grain size independently of the mineralogical content of each particle size component. Soil with particles diameters between 0.05 millimeters and 2 millimeters are called Sandy soils. Soils with particle diameters between 0.002 millimeters and 0.05 millimeters are termed as silts. Soils with particle diameters less than 0.002 millimeters are called clayey soils. Figure 2.1 shows the classification triangle for various types of soil and is useful as it allows an estimate of the clay content which often consists essentially of clay minerals which affect soil conductivity.

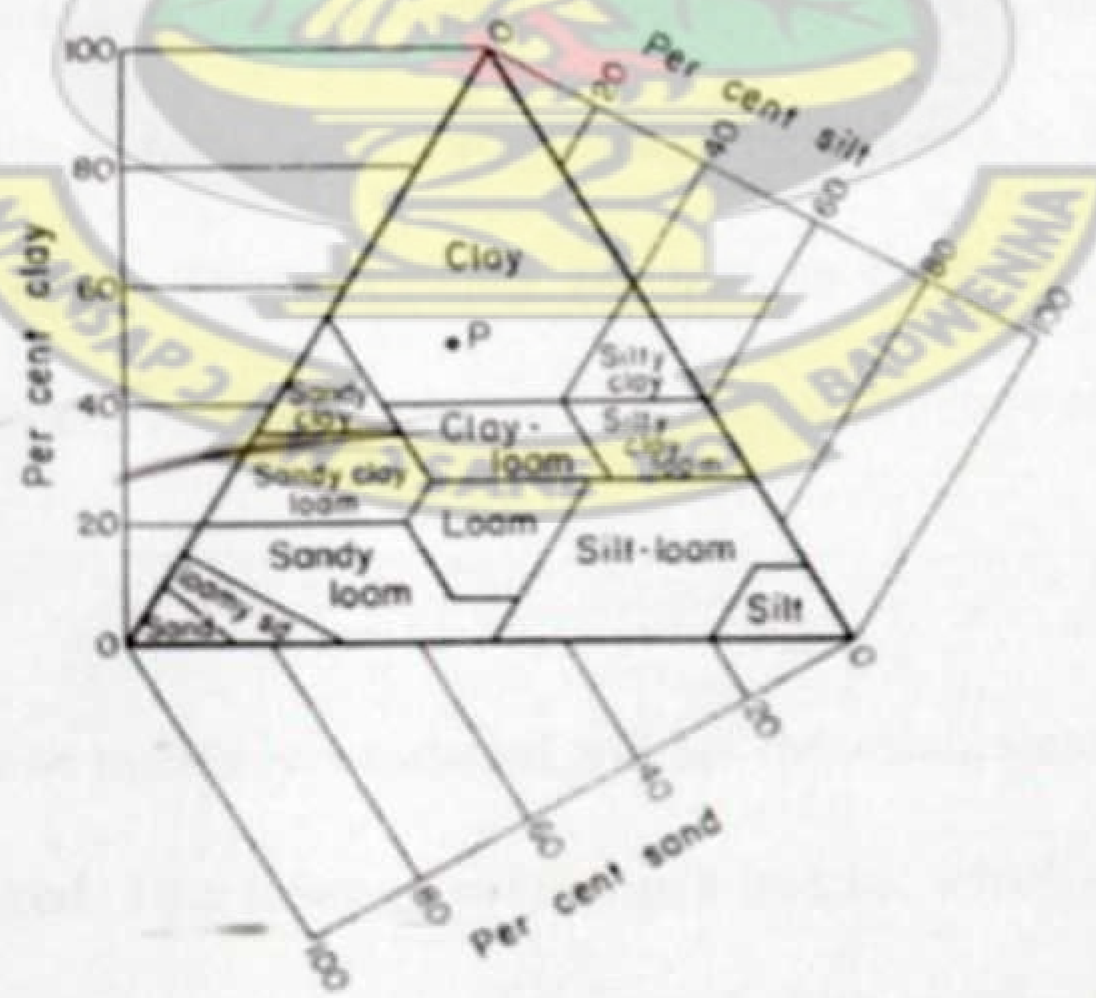


Figure 2.1 Agriculture textural classification triangle with axes added. The Point P represents clay (soil) containing 50 per cent clay, 20 percent silt and 30 percent sand (Kirkham, 1964) Geonics Ltd 1980 TN 5

The minerals in sand and silt fractions of the soil are electrically neutral and are generally excellent insulators (McNeil, 1980). But moist clay is a very good conductor. Clay consists of microscopically fine particles of minerals such as feldspar, mica, etc, the particles are so fine-grained that they are described as micro-crystals. During the formation of clay through weathering, positive charges (cations) are adsorbed to the surface. These cations (typically Ca, Mg, H, K, Na, $NH_3$) are loosely held to the surface and can be subsequently be exchanged for other cations or essentially go into solution should the clay be mixed with water (Keller, 1966).



**Organic Materials:** Organic materials are the remains of plant and animal life in the soil. These materials decay and accumulate to form a blackish material called humus (Weber). Little is known of the effects of humus on the electrical conductivity of soil (McNeil, 1980)



## 2.2 Soil Profile

According to Maxey (1964), , as long as there is rainfall and the temperatures are not too low there is a tendency for soils to form layered structure. A typical soil profile has three different horizons as one moves down. These horizons can vary in thickness from a centimeter to several meters or tens of meters and differ in colour, texture, structure and other properties.

The top horizon is the most intensely weathered and has the soluble minerals leached out and most other minerals altered. This layer contains much humus, which contributes to its dark colour. Structurally it is friable, granular, or platey much more so than the underlying horizon which is generally a zone of clay accumulation.

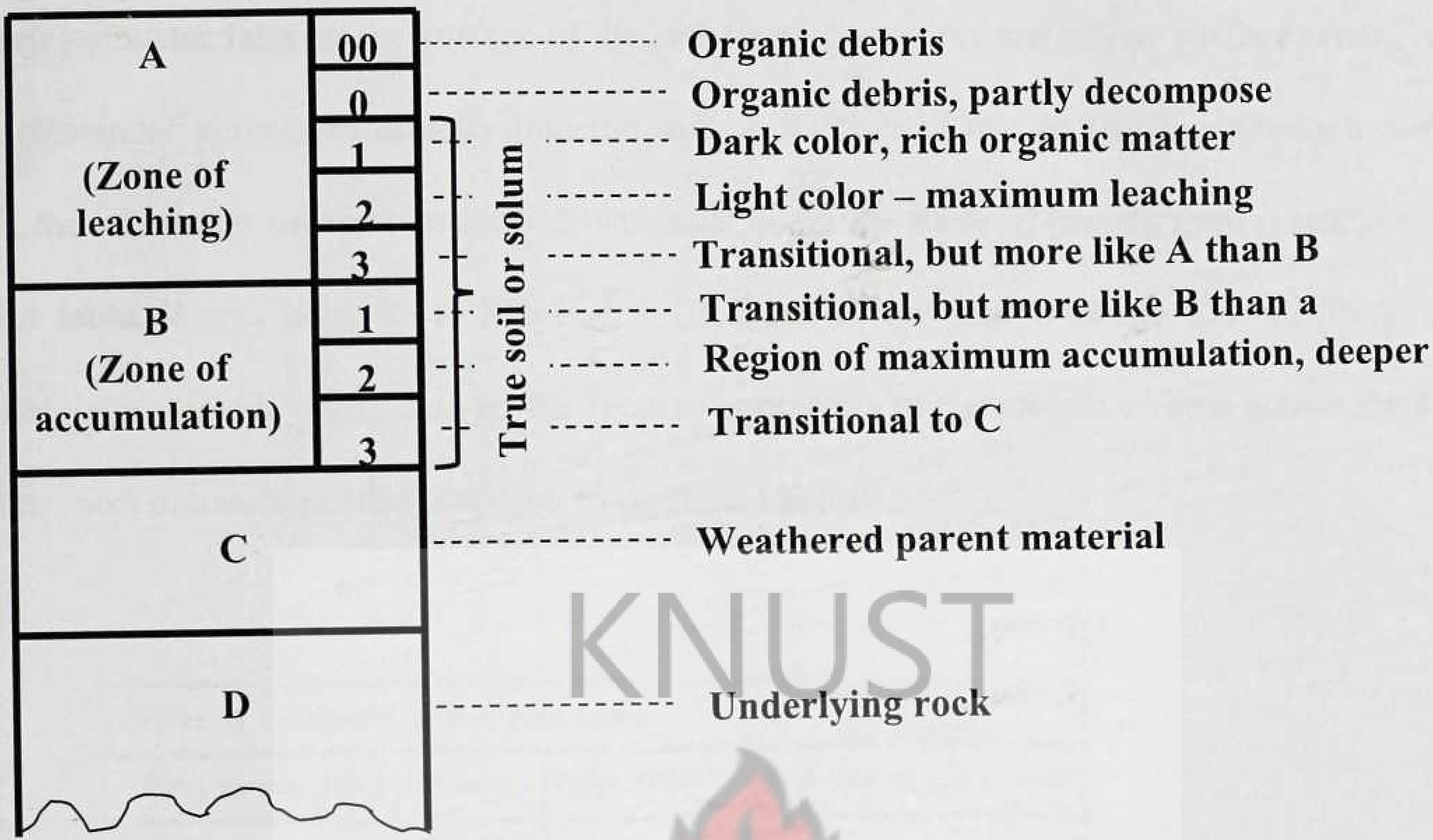


Figure 2.2 Normal or zonal soil profile (Maxey, 1964) Geonics Ltd 1980 TN 5

The next layer, called the zone of accumulation, generally displays a vertical structure in widely or closely spaced joints and it is this horizon that exerts the greatest influence on water movement vertically downwards. When the clay is dry these joints allow rapid downwards movement but when the clay is wet it expands and can close the joints to make the layer impermeable, which may in turn cause the top horizon to become saturated for appreciable periods of time. The third horizon consists of fless – weathered parent material and is usually relatively permeable (Maxey, 1964).

### 2.3 Soil Moisture and Groundwater

When rainwater falls on the surface of the soil fraction runs off directly as surface runoff and the remainder percolates directly into the soil. A fraction of this moisture is retained in the soil, the remainder moves vertically downwards under the force of gravity until it reaches the water table. Works done by P. Meyboom, 1967 has shown that there are four stages in the soil moisture profile depending on the relative continuity of the moisture films across the soil grains. Soil moisture profile is shown in figure 2.3 below.

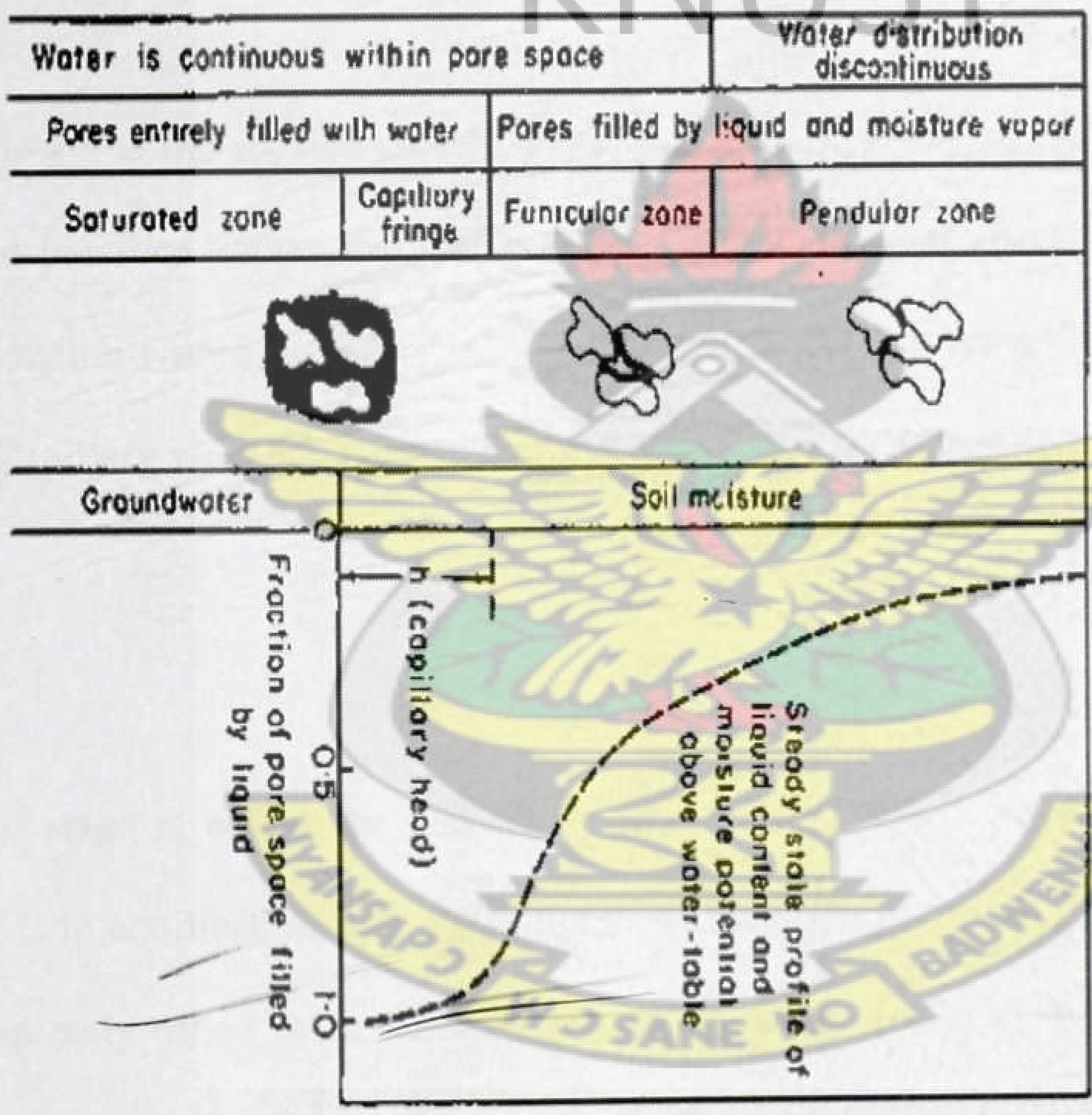


Figure 2.3 Liquid occurrences in soils (Meyboom, 1967) Geonics Ltd 1980 TN 5

In the uppermost region we have the pendular state in which the pore space is largely filled with water vapour. Actual liquid water exists only in very small isolated rings around the grains contacts and a continuous path does not exist between the various moisture occurrences.

At greater depth we have the funicular state in which the pendular rings have coalesced to the point where the liquid films have just become continuous throughout the pore space and entirely enclosed or encapsulated the vapour phase. At this depth the moisture path is now continuous.



Further down, is the capillary stage, all pore spaces at this stage are occupied by liquid but the liquid pressure within the pores is less than the total pressure caused by gravity since capillary action within the fine pore spaces has caused the moisture to ascend into these pore spaces. Capillary rise, determined effectively by pore size and type seldom exceeds several meters.

The final stage is called the phreatic surface (water table). At this stage the atmospheric pressure is in equilibrium with the hydrostatic pressure. All pores within the phreatic surface are completely filled with liquid under hydrostatic pressure and this is the region of groundwater, also known as the zone of saturation. The three regions above the phreatic surface are collectively referred to as soil moisture, suspended water, vadose water or zone of aeration.

Groundwater is free to move laterally with velocities ranging from a meter or more per day to less than a meter per year depending on the hydraulic pressure differential and the permeability of the material (Todd 1964). Studies show that soils with high clay content, high degree of compaction and small radius of soil pores decreases the saturated hydraulic conductivity of the groundwater.

Water table in general is not horizontal and is often a subdued version of the local topography.



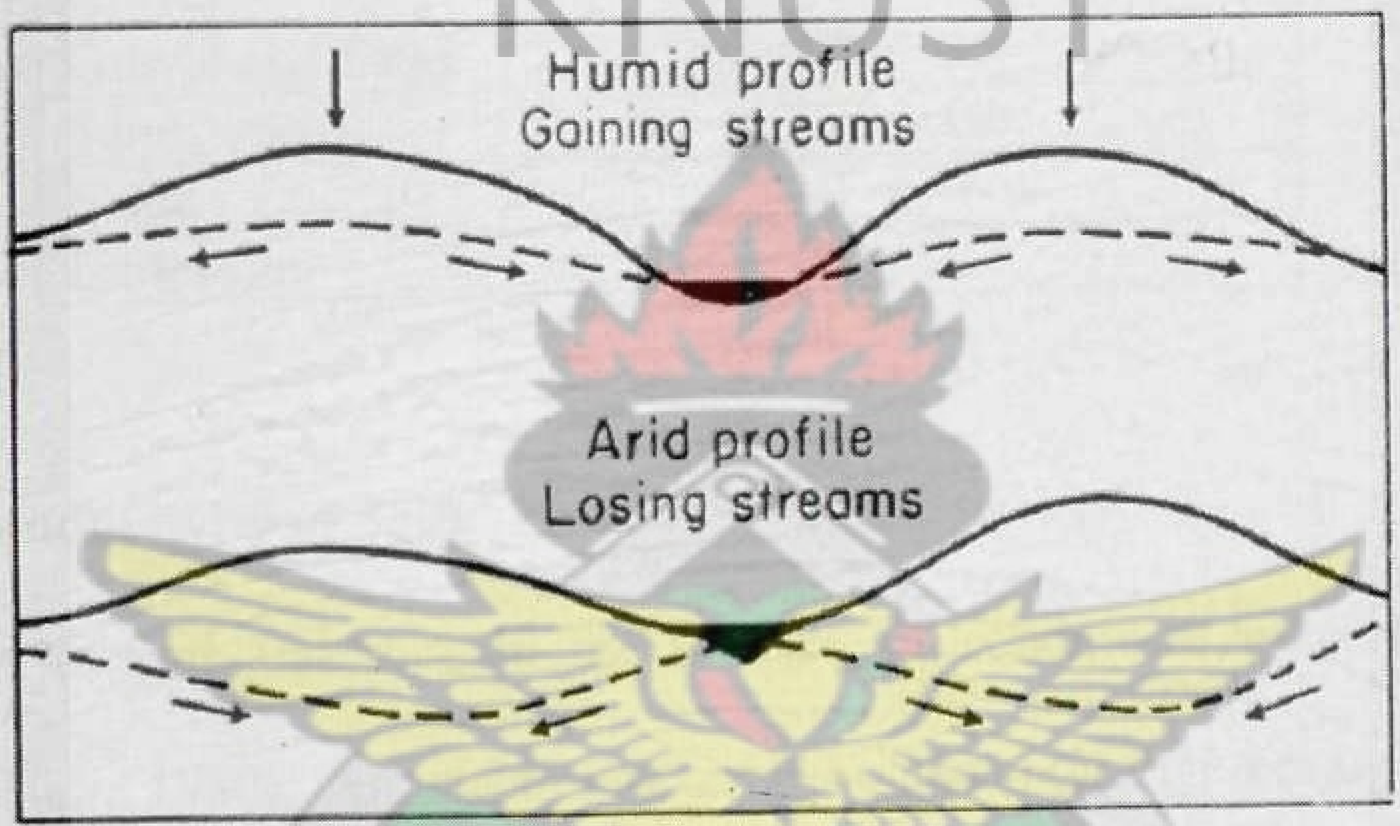


Figure 2.4 Profiles of water tables in arid and humid regions (Maxey, 1964) Geonics Ltd 1980 TN 5

Two example of water table in arid regions and in humid regions are shown in Figure 2.4. For Humid regions the moisture moves from topographic high regions down to the draining streams whereas in an arid region the moisture moves downwards away from the streams.

If all of the moisture in a soil sample is removed by drying, the ratio of the empty volume to the total volume of the soil matrix is known as the soil porosity (McNeil, 1980). The degree of compaction of soil affects the soil porosity. Table 2.1 below gives various types of soils and their percentage porosity ranges.

Table 2.1 Representative porosity ranges for sedimentary materials (Todd, 1964) Geonics Ltd 1980 TN 5

| Material | Porosity, % |
|---|---|
| Soils | 50 – 69 |
| Clay | 45 -55 |
| Silt | 40 – 50 |
| Medium to coarse mixed sand | 35 – 40 |
| Uniform sand | 30 – 40 |
| Fine to medium mixed sand | 30 – 35 |
| Gravel | 30 – 40 |
| Gravel and Sand | 20 – 35 |
| Sandstone | 10 – 20 |
| Shale | 1 – 10 |
| Limestone | 1 – 10 |



### 2.4 Electrical Conductivity of Soils

The conductivity of soil and rock in the absence of conductive minerals is principally electrolytic (McNeil, 1980). An electrolyte is any substance that produces ions when it dissolves in water. The conductivity of an electrolyte is proportional to both the total number of charge carries (ions) in solution and their velocity. The velocity also depends on the viscosity of the solution which is also a function of temperature. The dependence of water conductivity based on the amount of ions present is illustrated in table 2.2 which shows the calculated measured conductivity of three lakes, (Lake Erie, Lake Huron and Lake Superior) based on various ions found in them and its correlation with the actual measured conductivity of each lake (Doherty, 1963)

Table 2.2 Conductivity of Great Lakes with contribution of the various ions (L.H. Doherty) Geonics Ltd 1980 TN 5

| Ion | Lake Erie | Lake Huron | Lake Superior |
|---|---|---|---|
| HCO | 5.8 | 4.1 | 2.6 |
| Ca | 10.1 | 7.3 | 3.8 |
| Mg | 3.6 | 3.2 | 2.4 |
| Na | 1.8 | 0.6 | 0.2 |
| Cl | 3.9 | 1.2 | 0.2 |
| SO | 3.4 | 1.8 | 0.3 |
| Calculated Conductivity (mmhos/m) | 28.6 | 18.2 | 9.5 |
| Measured Conductivity (mmhos/m) | 26.7 | 18.2 | 8.4 |

The table below, 9Table 2.3) developed by (Heiland, 1968) illustrates typical values of conductivity of various natural water sources.



Table 2.3 Typical values of conductivity of various natural water sources (Heiland, 1968) Geonics Ltd 1980 TN 5

| Natural Source | mS/m |
|---|---|
| Meteoric waters (from precipitation) | 1 – 30 |
| Surface waters (lakes and rivers) | 0.3 for every pure waters, 10,000 for salt lakes, 2-30 in igneous regions, 10 – 100 in sedimentary regions |
| Soil Waters | Up to 10,000 average around 10 |
| Groundwater | 6 to 30 in igneous regions, 1000 in sedimentary regions |
| Mine waters (copper, zinc, etc. sulphates) | Not usually less than 3000 |

**2.5 Groundwater Contamination**

Groundwater not only contains the hydrogen and oxygen atoms that form water ($H_2O$), but it also contains naturally dissolved gases from the atmosphere and dissolved minerals and gases from the soil and rock through which it passes. According to WHO usage (WHO, 2006), groundwater contamination is defined as the introduction into water of any substance in undesirable concentration not normally present in water, e.g. microorganisms, chemicals, waste or sewage, which renders the water unfit for its intended use.

The soil filters the water and absorbs and removes many contaminants though some will pass through unimpeded. But if the soil layer is thin, has high permeability, or if the water table is close to the land surface, then the soil is less likely to adequately treat contamination. The excess contaminants may pass through the zone of aeration and enter the groundwater in the zone of saturation. If this happens, a plume forms. A plume is an underground pattern of contaminant concentrations created by the movement of groundwater beneath a contaminant source. The contaminant spreads mostly laterally in the direction of groundwater movement (Figure 2.5). The site of original contamination has the highest concentration of contaminant and the concentration decreases as it moves further away from the source.



**Plume Contamination**

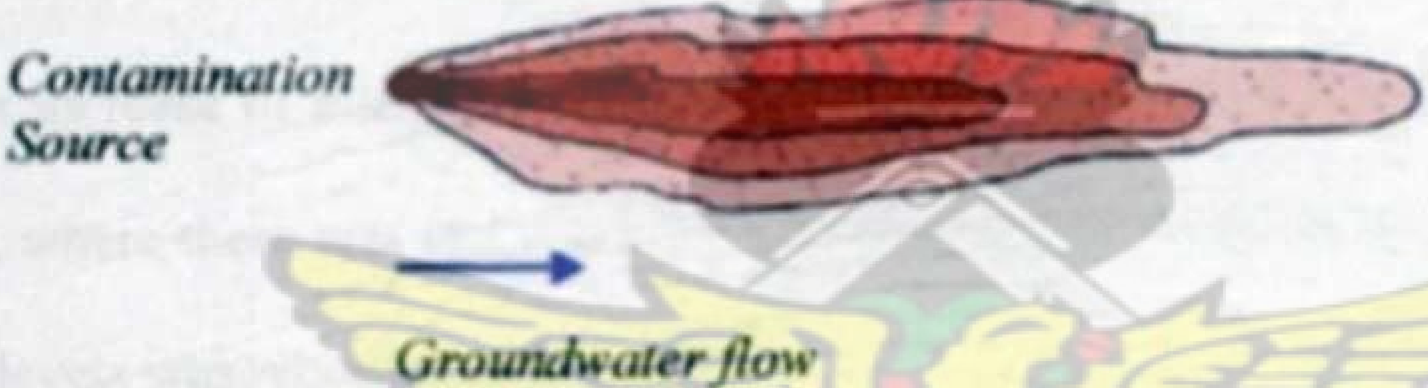


Figure 2.5 Plume contamination flow in ground water.

Groundwater contamination can be from natural sources or from man-made activities or both (Duah, 2006). Groundwater gets naturally contaminated as a result of their interaction with soils and rocks in which they are found. A monitory programme undertaken by the regional Ghana Water and Sewage Cooperation Laboratory in Tamale on 93 boreholes and shallow well water supply sources in the region indicated that about 63.5 percent of the wells had fluoride concentrations in excess of 1.0 mg/l. The problem has been attributed to the geology of the area i.e. Bongo granite (Smedley et al, 1994).

Man-made sources of groundwater contamination include, poorly designed hazardous waste disposal facilities e.g. unlined landfills or open damps, leakages from underground storage tanks, liquid spills and discharges from mining companies and excessive use of pesticides and fertilizers in agriculture. In Ghana the main man-made source of groundwater contamination is mainly due to agricultural practices and mining activities (Duah, 2006). The main chemical contaminant from mining activities is Arsenic. Research undertaken between 1992 and 1995 by Water Resources Research Institute indicates high concentration of Arsenic in water from streams, shallow wells boreholes in Obuasi, which has one of the biggest mines in Ghana.



Surveys conducted in the upper east region of Ghana in 1969, 1977 and 1980 indicate a significant increase of nitrate levels in groundwater between 1977 and 1980. Between 1959 and 1977, where there was not much agricultural activity in the area no appreciable increase in nitrate levels was recorded (Akiti, 1982).

Landfills are another major source of soil and water contamination. Landfills are the places that garbage is taken to be buried. Landfills are supposed to have protective bottom layers to prevent contaminants from getting into the groundwater. However, if there are no preventive layers or these layers are breached, contaminants in the form of leachate from deposited waste materials like car battery acid, paint, household cleaners, etc. can make their way down into the groundwater. Landfills in Ghana are primarily open dumps without leachate or gas recovery systems (Mensah et al, 2005). Literature on the impact of these landfills on its surrounding environment especially groundwater is difficult to come by though they pose a major threat to their host environment.

## 2.6 Landfills

A landfill is a designated site where waste is deposited or buried. Landfills are usually designed to bury waste but not to break them down. Engineered sanitary landfills have well controlled highly engineered containment systems to minimize the impact of solid waste disposal on the environment and on human health (Kerry et al, 2005).

## 2.7 Engineered Sanitary Landfill Design



As mentioned earlier, Engineered Sanitary Landfills have well controlled, highly engineered containment systems designed to minimize the impact of solid waste disposal on the environment. This highly controlled containment systems are achieved by the use of liners and other containment mechanisms.

Landfill liners are applied on landfills to provide a barrier to minimize migration of leachate from the containments site to adjoining groundwater. This is normally achieved by installing a liner system at the base and sides of the landfill. The commonest materials used as landfill liners are compacted clay and geomembrane (Figure 2.6). Other materials such as compacted compost can be used because according to research conducted by Benson and Othman (1993) it displays hydraulic and mechanical properties required for liners. However, contaminants such as heavy metals were found to leach from the compacted compost (Benson and Othman 1993), which is a disadvantage.

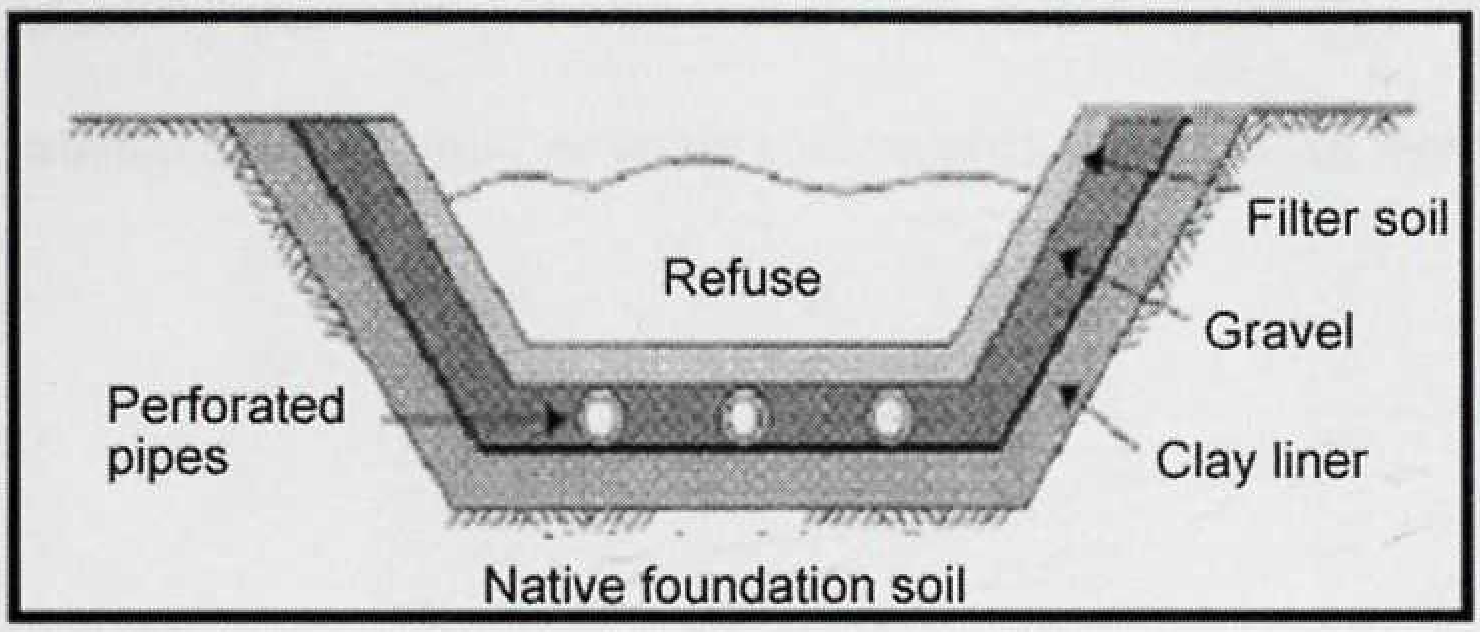


Figure 2.6 Cross- sectional view of compacted clay

Combined liner systems, known as composite lining (Figure 2.7), is far more effective than single liners (Bouazza and Van Imp, 1998). Leachate collection in a landfill is achieved by inserting perforated pipes inside the liners.

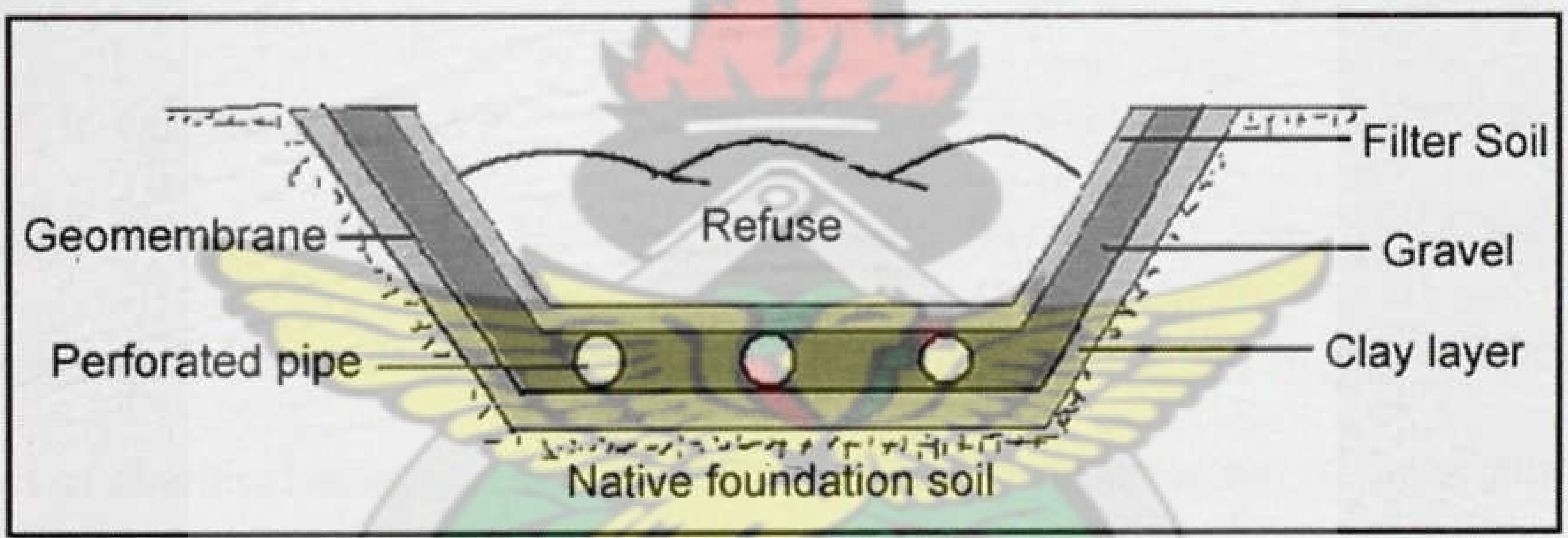


Figure 2.7 Cross – sectional view of a composite liner

**2.8 Leachate Generation**

Solid wastes disposed off at landfills undergo physical, chemical and microbial changes (Christensen et al, 2001). These processes make the waste water soluble and are easily washed and dissolved by percolating water (Bjerg et al. 2003).

Landfill leachate is formed when excess water percolates through the waste layers (Christensen et al, 2001), thus removing the soluble contaminant compounds from the solid waste. The sources of percolating water include precipitation, irrigation, surface runoff, groundwater intrusion and the initial moisture content present within the waste (El-Fade et al, 2002).

### 2.9 Leachate Plumes

According to research done by Freeze and Cherry in 1979, infiltration of water through a landfill waste will normally cause water table build-up within and below the landfill, this is known as mounding.



Mounding causes leachate to move vertically (downwards) and laterally (outward) as shown in Figure 2.8. In cases where the base of the landfill is not lined with a hydraulic barrier and also if the underlying soil profile is highly permeable the vertical flow of leachate may contaminate groundwater resources. The seeping of leachate into groundwater will normally result in a set of chemical reactions that change the chemical composition of the groundwater (Acworth, 2006). The leachate that flows laterally normally gather around the landfill giving rise to leachate spring or may seep into surface water bodies

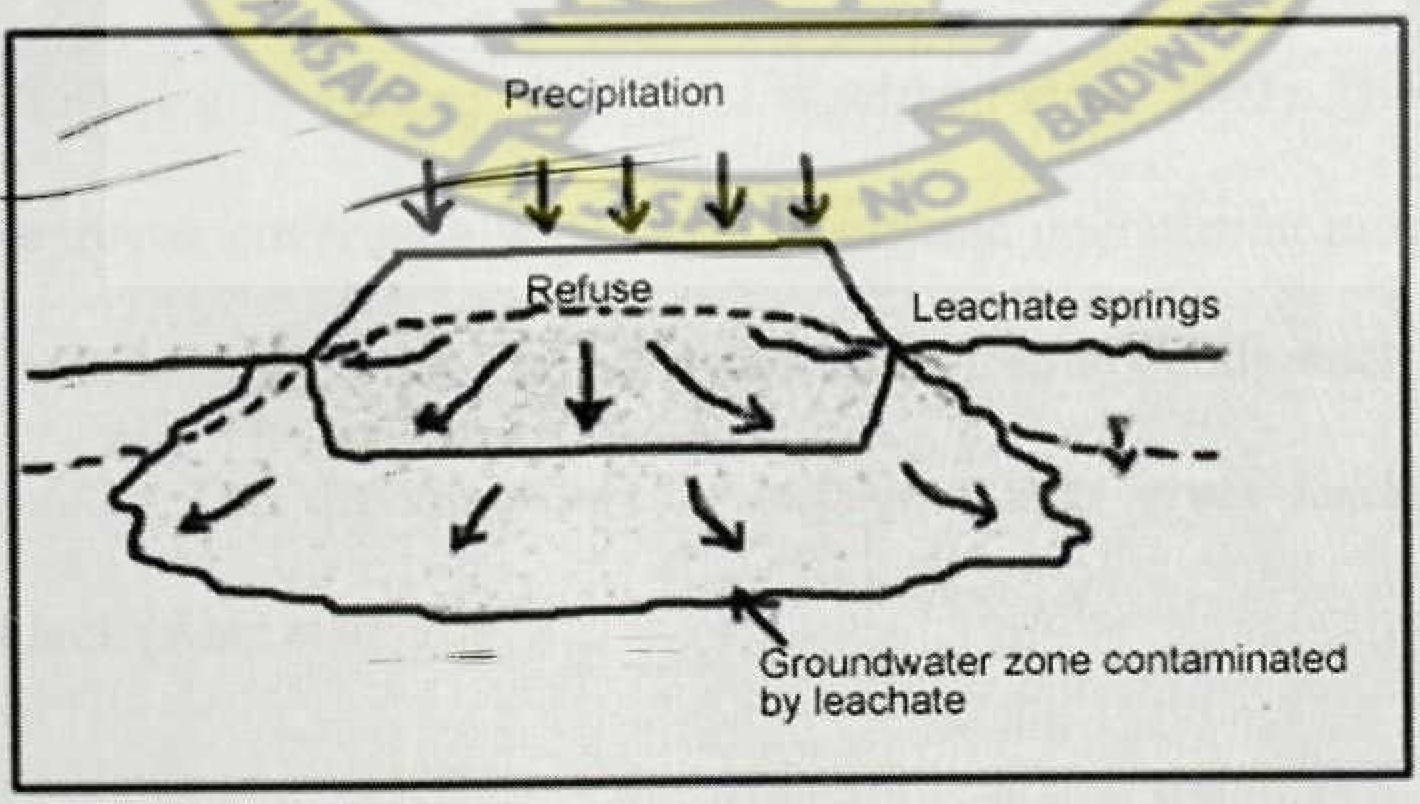


Figure 2.8 Leachate mound and movement beneath a landfill

The plume normally has concentrations of various chemical constituents which are much higher than those present in the pristine groundwater. In one study Nicholson et al. (1983) reported calcium to be the dominant cation and sulphate and bicarbonate to be the dominant anions in the leachate contaminant plume with maximum concentrations of 400, 2000 and 1200 $mgl^{-1}$ respectively.

## 2.10 Leachate chemical characteristics

Most sanitary landfills normally receive a mixture of municipal, commercial and mixed industrial waste. These do not include hazardous, radioactive, and specific chemical wastes. Leachate generated from such landfills may be characterized on the basis of four major groups of pollutants, namely dissolved organic matter, inorganic macro-components, heavy metals and xenobiotic organic compounds (Christensen et al. 1994).

The dissolved organic matter component of landfill leachate is usually expressed as Chemical Oxygen Demand (COD), Total Organic Carbon (TOC) or Biochemical Oxygen Demand (BOD). At early stages of landfilling, leachate usually has high BOD (e.g. 9500 $mg.l^{-1}$) value and even higher COD (e.g.14 000$mg.l^{-1}$) content (Kjeldsen et al. 2002). Dissolved organic matter is a bulk parameter covering a wide range of organic degradation products including methane ($CH4$), volatile fatty acids and some refractory compounds such as fulvic and humic-like compounds. The decomposition of organic matter gives leachate its colour: yellow, brown or black (Aziz et al. 2007).

Major inorganic constituents of leachate are: calcium (Ca), magnesium (Mg), sodium (Na), potassium (K), ammonium $(NH_4^+)$, iron (Fe), manganese (Mn), chloride ($Cl^-$), sulphates $(SO_4^{-2})$ and bicarbonates $(HCO_3^-)$. The concentrations of most of the macro components in leachate depend on the stabilization processes in the landfill (Kjeldsen et al. 2002).

Heavy metals include arsenic, cadmium, chromium, cobalt, copper, lead, mercury, nickel and zinc. Most heavy metals occur naturally as ores, in the environment. Anthropogenic sources of heavy metals are usually deposited in landfills as refuse. Concentrations of heavy metals in landfill leachates are normally low and do not pose a groundwater pollution problem at landfills (Bjerg et al. 2003). However, if present in high concentrations, heavy metals can cause leachate to be toxic (Sawaittayothin and Polprasert 2007).



**2.11 Methods of Leachate plume detection**

The traditional method of detecting leachate plumes in groundwater around a landfill is to have groundwater sampling points installed down - gradient. Hydrochemical parameters such as chlorides, sulphates and electrical conductivity (MacFarlane et al., 1983) are used to examine the extent of contamination in the sampled groundwater. The first challenge in using this method is the cost of drilling, secondly if the borehole is not well positioned it may fail to give ~~the overall~~ nature of the groundwater and thirdly there are usually inadequate number of these boreholes.

In the light of these challenges geophysical methods in the past years have also been used as reconnaissance tool to characterize the subsurface around hazardous waste sites (Porsani et al., 2004). The next sections present a number of geophysical methods and how they have been used to solve environmental problems, and their suitability to solve groundwater contamination problems.

## 2.12 Application of Geophysical Techniques for leachate detection

### 2.12.1 Introduction

Surface geophysics is used to define natural conditions and man-made features that may contain hazardous waste or influence the movement of contaminants. While the range of environmental problems is very broad, they typically involve the need to determine the location and nature of fixed or mobile environmental hazards. Fixed hazards like buried waste containers and mobile hazards such as spilled contaminants or fluids leaking from tanks or barrels.

Although the nature of environmental problems is typically different from traditional resource exploration targets, geophysical techniques can often provide a noninvasive means of obtaining the information required to characterize a site, be it a landfill or other hazardous or toxic waste site.

In the characterization of mobile hazards, geophysical techniques are usually used to determine the following, geologic zones and boundaries that control fluid flow, fractures that control flow in crystalline rocks, inorganic contaminant plumes that may originate from industrial operations, landfills, or abandoned mines, saltwater intrusion in aquifers and abandoned wells which can serve as conduits for contaminant transport.

A survey of current applications demonstrates the wide range of problems that are being addressed by geophysical techniques. The next section synthesises a number of geophysical methods that are being used to solve such and related environmental problems.

The most applied geophysical method in groundwater contamination studies are electrical resistivity, electromagnetic and ground penetrating radar. These techniques are applied in landfill investigations because dissolved plume (leachate) can influence resistivity/conductivity, dielectric constant.



### 2.12.2 Electrical Resistivity

In this method electrical currents are injected into the ground by the use of direct contact electrodes. The method operate using direct current (DC) of low frequencies

This method utilizes the different electrical resistivities of minerals, rocks and domestic waste deposits. Direct-current (DC) electrical resistivity method for conducting a vertical electrical sounding (VES) is very popular with groundwater studies due to the simplicity of the technique and the ruggedness of the instrumentation. An excellent example of the use of the technique was shown by Reynolds (1997) in a survey for a rural water supply in Northern Nigeria. Van Overmeeren (1989) showed the use of electrical measurements in mapping boundary conditions in an aquifer system in Yemen. Beeson and Jones (1988), Olayinka and Barker (1990), Hazell et al. (1988 and 1992), Barker et al. (1992) and Carruthers and Smith (1992) all have demonstrated the use of electrical techniques for siting wells and boreholes in crystalline basement aquifers throughout sub-Saharan Africa. Other similar examples are given by Wurmstich et al. (1994), Yang (1998), and Yang et al. (1994), who demonstrated a useful development of electrical techniques by considering the conductance of the DC section as a guide to overall aquifer potential for mapping groundwater resources in the Kalahari Basin.

### 2.12.3 Ground Penetrating Radar

GPR uses high frequency electromagnetic waves (radar) to acquire subsurface information. The waves are radiated into the subsurface by an emitting antenna. When a wave strikes a material with dielectric constant different from that of the propagating medium, a portion of the wave is reflected back to a receiving antenna where its travel time is measured. The water table is often also a strong GPR reflector, as shown by the work of Trenholm and Bentley (1998), which can limit the penetration depth of the signals.

Greenhouse et al. (1997) have given good examples of the use of GPR in conjunction with VLF and FDEM at sites near Ontario, Canada. At one site near the city of Ontario a contaminant plume from a landfill was further described by Cosgrave et al (1987) who showed that where the background conductivity is low the method provides a means of monitoring contaminant plume flowing through glaciolacustrine sands

Other important work has been done with the use of GPR to produce 3D images of the subsurface (Roberts et al, 1992), however once again, this use within groundwater studies is likely to be cost prohibitive.

### 2.12.4 Electromagnetic Induction Survey

In this method a transmitter coil radiates an electromagnetic field which induces eddy currents in the subsurface. The eddy currents, in turn, induce a secondary electromagnetic field. The secondary field is then intercepted by a receiver coil. The voltage measured in the receiver coil is related to the subsurface conductivity.

Electromagnetic Induction techniques have been extensively developed and adapted over the years to map lateral and vertical changes in groundwater conductivity. There are two types of electromagnetic survey currently practiced, Time Domain Electromagnetic (TDEM) surveys which are mainly used for depth soundings and frequency domain electromagnetic (FDEM) surveys that are used mostly for mapping lateral changes in conductivity

The two electromagnetic techniques (TDEM and FDEM) that measure the conductivity of the ground by inducing an electric field through the use of time varying electrical currents in transmitter coils located above the surface of the ground. These time -varying currents create magnetic fields that propagate in the earth and cause secondary electrical currents which can be measured either while the primary field is transmitting (during frequency domain surveys) or after the primary field has been switched off (for time domain surveys).

Frequency- domain Electomagnetics (FDEM) technique is usually used to measure lateral conductivity variations along line profiles either as single lines or grids of data. Further recent improvements in FDEM have seen the integration of GPS technology with the FDEM instruments which has led to a dramatic increase in the rate at which electromagnetic surveys can be accomplished. A number of manufacturers offer FDEM equipment that varies in physical size, ease of operation and survey depth. An example is Geonics Ltd. electromagnetic equipment EM34-3.

Typically survey results for FDEM surveys are presented as contour maps of conductivity and 2D geo-electric sections showing differences in conductivity along a line profile. Changes in conductivity are often associated with differences between lithological sequences and over disturbed ground such as faulted or mineralised zones.



A useful example of FDEM for groundwater studies has been given by Godio et al. (1998) in a mountainous area in North-Eastern Italy. Here a frequency domain survey using 20 m and 40 m coil separations gave information on the electrical resistivity for locating a number of water wells.

Hoekstra and Blohm (1990) used TDEM to map different levels of saltwater intrusion into three different aquifers near Monteray Bay, California. The increase in total dissolved solids in the fluid showed the progress of saltwater intrusion where the deepest aquifer had the least amount of abstraction and was least intruded by the saltwater. The shallowest aquifer, with greatest abstraction rates, showed the greatest salt water intrusion inland. Hild et al. (1996) used a similar approach to map the fresh water lens floating on the saltwater beneath the island of Guam in the Northern Mariana Islands, western Pacific. This approach has seen much success in these types of groundwater exploration projects (Hild et al., 1996). In these types of studies use is made of the Ghyben-Herzberg principal (Davis et al, 1966) where a basal lens of fresh water floating on denser salt water has a thickness which forces the freshwater-saline water contact to a depth below sea level that is 40 times the elevation of the top of fresh water above sea level. The fresh water/saline water boundary shows a high electrical contrast that is easily mapped with TDEM techniques especially in resistive bedrock. This freshwater resource is a significant one for many of these islands where water storage is poor and water demand is on the increase.

Maimone et al. (1989) demonstrated the use of TDEM in urban areas for mapping the freshwater-saline water boundary with surveys around Southern Nassau County, Long Island NY. The use of TDEM for mapping other groundwater systems includes that for karstic aquifers (Alwail, 1996), work on small pacific islands (Hild et al., 1996), integration with borehole data (Paillet et al., 1999) and investigations of block-faulted terrains (Petersen et al., 1989).

The successful use of TDEM in arid environments is also demonstrated by the work of Young et al. (1998) in Oman where over 30% of the population rely on groundwater extracted from alluvium aquifers on the Batinah Plain on the coast of the Gulf of Oman. Their work along over 400 km of profiles defined three zones within the aquifer and a wedge of saline intrusion up to 10 km from the coast. Taylor et al., (1992) showed the use of TDEM with simple 1D, closely spaced soundings to define local hydrogeology in an arid alluvial environment near Reno, Nevada. The results were used to reduce the total number of wells required to characterize the groundwater system.

The main use of magnetic techniques for groundwater investigations has been as part of combined surveys with gravity for defining large -scale basin structures. Babu et al (1991) used magnetic techniques in mapping bedrock topography and groundwater reservoirs in igneous and metamorphic rocks. Magnetic surveys are also often used to locate the cause of contaminated groundwater by surveying for buried metallic objects such as hydrocarbon storage tanks and chemical containers.

# CHAPTER THREE

# THEORY, SITE DESCRIPTION AND GEOPHYSICAL SURVEY

## 3.1 Theory of Electromagnetic Induction

The FDEM induction method is based on the response of an induced alternating current in the ground. In figure 3.1 consider a transmitter coil *T*x energized with an alternating current at an audio frequency placed on the Earth, and a receiver coil *R*x located a distance away. The time-varying magnetic field *Hp* arising from the alternating current in the transmitter coil can induce very small currents in the subsurface conductor. These currents generate a secondary magnetic field *Hs*, which is sensed by the receiver coil, together with the primary field, *Hp*.

The instrument output, calibrated to read in units of terrain conductivity (apparent conductivity), is obtained by comparing the strength of the quadrature phase component of the secondary field to the strength of the primary field. The apparent conductivity measurement represents a weighted average.

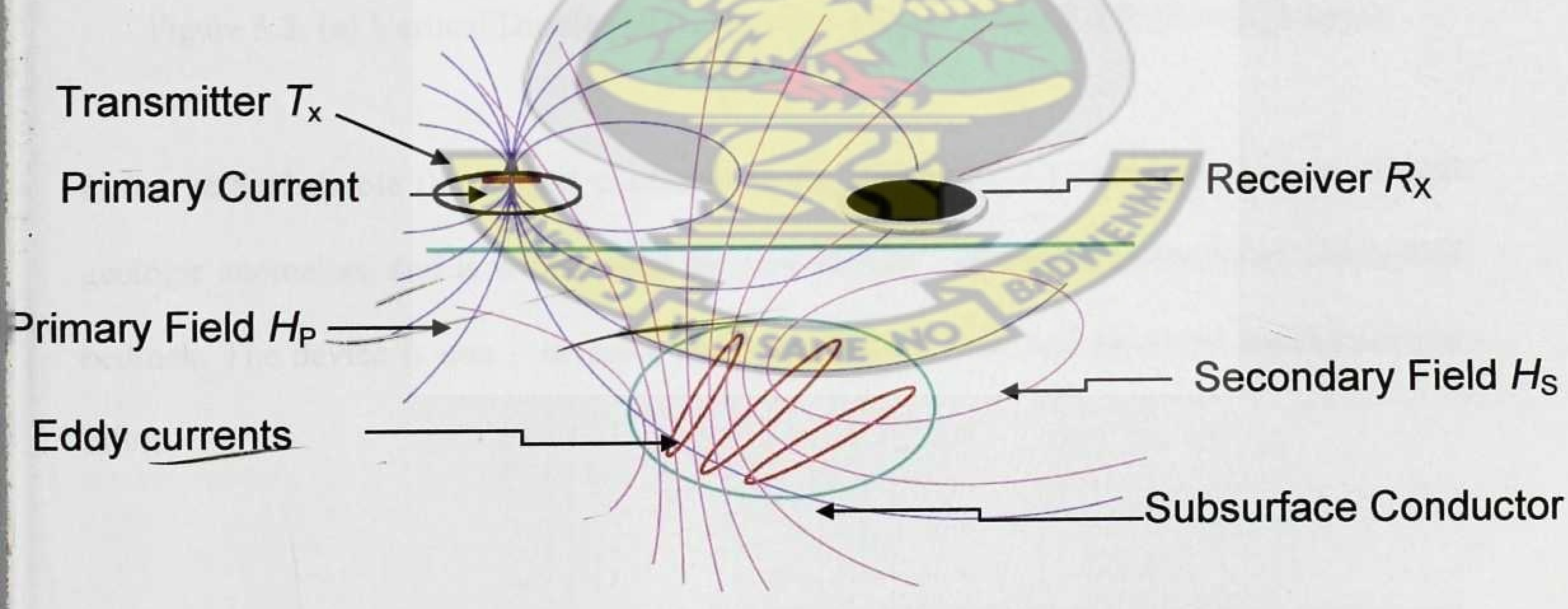


Figure 3.1Electromagnetic Induction Process

### 3.2 Instrumentation for Geophysical Survey – *The Geonics EM 34-3*

In this investigation an EM ground conductivity survey was done using Geonics EM34-3 instrument. This instrument is designed and manufactured by GEONICS Limited Ontario, Canada. The instrument consists of insulated transmitter and receiver coils with equal internal diameters of 63 cm. The EM34-3 uses three intercoil spacings -10, 20 and 40 m to provide variable depths of exploration down to 60 metres. There are two main modes of operation: in the first mode (horizontal dipole mode, HDM) both coils, the transmitter and receiver, are located vertically; in the second mode (vertical dipole mode, VDM) the coils lie horizontally, on the surface (Fig. 3.2).



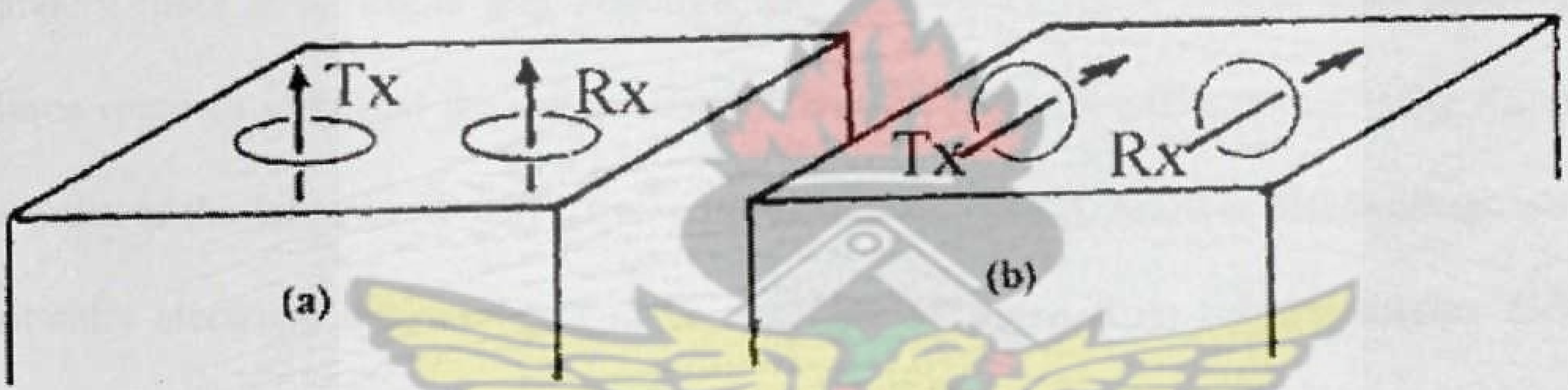


Figure 3.2: (a) Vertical Dipole (VD) and (b) Horizontal Dipole (HD) Configurations (McNeil, 1980)

In the vertical dipole (horizontal coplanar) mode, the EM34-3 is very sensitive to vertical geologic anomalies, and is widely used for groundwater exploration in fractured and faulted bedrock. The device is non – invasive and measures the bulk soil electrical conductivity in mS/m.

The advantages of using EM34-3 is that readings take less time about five seconds per location and readings can be recorded by a data-logger connected to the instrument or written in field notebook. Another advantage is that, when using the EM34-3 in horizontal dipole mode secondary magnetic field is in maximum coupling with the receiver coil and the measurement is relatively insensitive to misalignment of the two coils. Furthermore since the depth of exploration is not as great as in the vertical dipole mode the indicated apparent conductivity stays linear with true conductivity to much higher values of conductivity, This feature is of particular importance when making measurements in very conductive regions, such as in mapping soil salinity (McNeil, 1985).

A disadvantage of operating in the horizontal dipole mode is the high sensitivity to near-surface conductivity since variations in this conductivity can mask changes at greater depths. Fortunately there is a simple and effective way of altering the response with depth. The technique requires only that the ground conductivity be laterally uniform to a radial distance of the order of the largest intercoil spacing used (McNeil, 1985). Another disadvantage is that occasionally electrical interference will be encountered, either from cultural sources (50/60 Hz power lines, industrial noise) or from atmospheric electricity (spherics). Noise from cultural sources will often manifest itself as a slow variation in the output meter reading and these variations must be averaged out by the receiver operator (McNeil 1980).

According to GEONICS Technical Note 6 (TN6) it can be shown under certain constraints (technically defined as operation at low values of induction numbers) that the secondary magnetic field is given by (expression derived completely in appendix B)

$$\frac{H_S}{H_P} \cong \frac{i\omega\mu_o\sigma s^2}{4} \qquad (1)$$

This equation is incorporated in the design of the Geonics EM34-3 equipment. This makes it possible to construct linear terrain conductivity meter to give a direct reading by simply measuring this ratio (Veil, 2005).

Given the ratio $\frac{H_S}{H_P}$ the apparent conductivity indicated by the instrument is defined from the equation (1) as

$$\sigma_a = \frac{4}{\omega\mu_o s^2}\left(\frac{H_s}{H_p}\right) \quad (2)$$



This gives the apparent conductivity, $\sigma_a$ in terms of the frequency, $f$ and intercoil spacing, $s$. Therefore, the ratio of the secondary magnetic field to the primary magnetic field is linearly proportional to the apparent conductivity. Hence, measurements taken under the conditions of low induction numbers provide an apparent terrain conductivity, $\sigma_a$ which the EM34-3 equipment reads directly.

### 3.3 Location and Description of Study Site

The Kumasi Sanitary Landfill and Septage treatment facility is located at Dompoase a suburb in Kumasi. The facility was established under the World Bank financed Urban Environmental Sanitation Project (Urban IV), and the Governments of Ghana, under the Ministry of Local Government Urban Environmental Sanitation Project. It commenced in January 2004. The facility is designed to handle both solid waste and septage produced in the city of Kumasi. The site is bordered on the south by the Oda River. The site has an overall area of 40 hectares (400000 $m^2$).

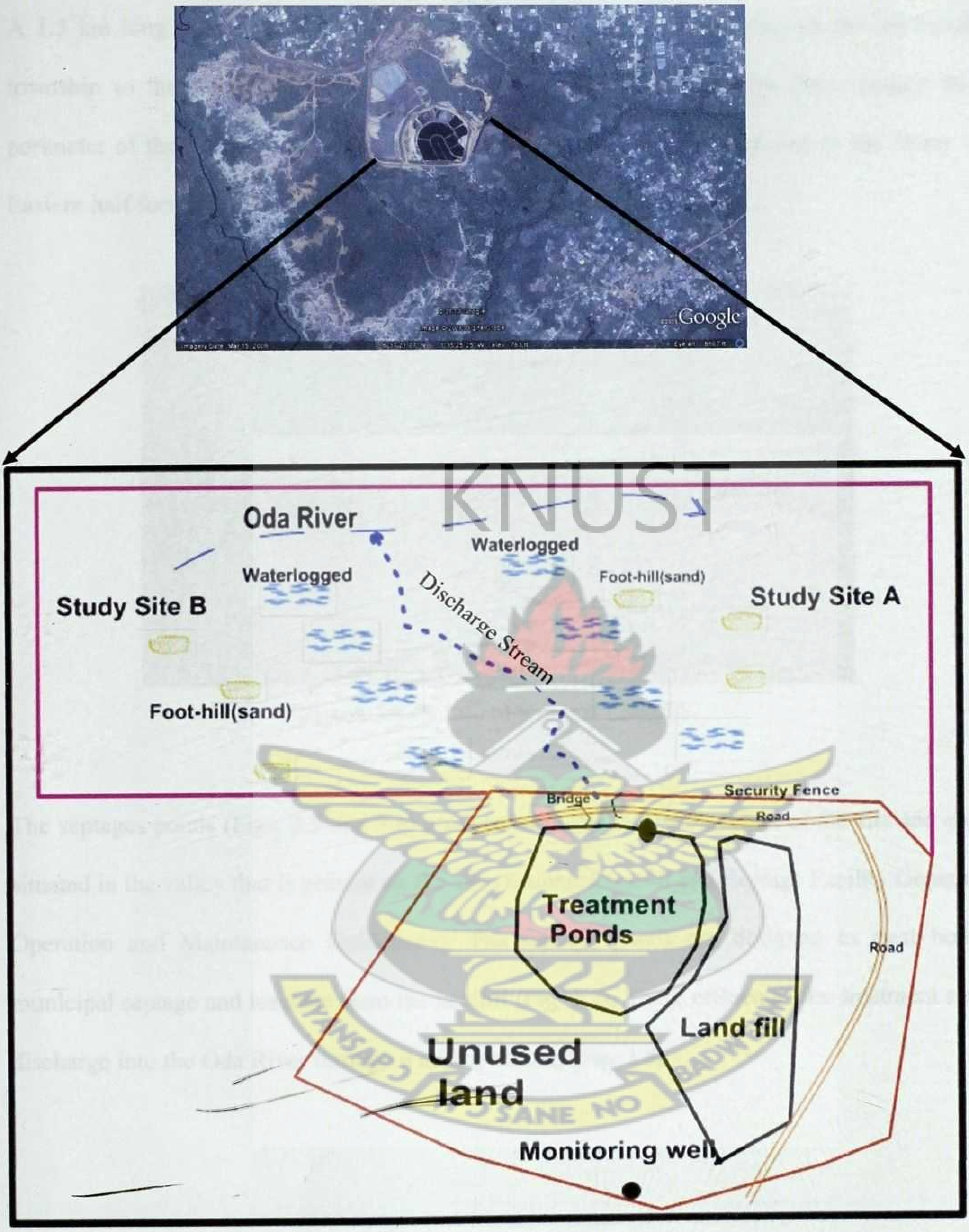




Figure 3.3 Location and map of Kumasi Landfill and Septic waste Treatment Facility

A 1.5 km long access road to the landfill links the Dompoase road through the industrial township to the North-Western corner of the site. There is a security fence around the perimeter of the site. The landfilling area is a valley, with a mound located in the North – Eastern half forming a smaller separate catchment area (Fig, 3.4).

Figure 3.4 Picture of Kumasi Landfill

The septages ponds (Figs. 3.5 and 3.6) are located at the lowest elevation of the site and are situated in the valley that is present on the site (Kumasi Landfill and Septage Facility General Operation and Maintenance Guidelines). The septage ponds are designed to treat both municipal septage and leachate from the landfill (Fig. 3.7). These effluents after treatment are discharge into the Oda River through a nearby stream (Fig. 3.8).


Figure 3.5 Picture of septic waste being discharged into the septic and leachate treatment ponds




Figure 3.6 Picture of septic waste treatment ponds

The facilities have 15-year design life to cater for the current daily generations rates of 860 tons Solid Waste and 500 cubic metres Fecal Sludge including the projected future increases after which new facilities would be required (Mensah *et al.*, 2003).

Figure 3.7 Picture of leachate discharge from landfill



Figure 3.8 Picture of liquid discharge from treatment ponds

### 3.4 Geology of Study Site

The Kumasi area is underlain by rocks of the Lower Birimian System, consisting principally of phyllites, greywackes and schist, intruded in places by quartz veins and stringers and massive granitic batholiths which are in turn often cut by pegmatite veins. A substantial part

Geology at and around the Kumasi Landfill and Septage Facility is described by Murray (1961) as lying within the Kumasi granitic batholiths, which is a post-Birimian intrusive of Precambrian age. The project site is covered by lateritic soil which is essentially a product of intense chemical weathering of the underlying granitic bedrock. These consist mainly of sand to silt sized quartz particles in a matrix of clay formed from the weathering of the feldspar constituents of the granitic rock. These soils also occasionally have a mica content which is a function of the degree of weathering and the amount of mica in the parent rock. Where the weathered soil profile is located in a valley, and subjected to the availability of water, the fines are sometimes leached out of the soil profile leaving deposits of relatively clean quartz sand and gravel. There is sand wining approximately 300 m from the project site. No major geologic discontinuities such as faults and shear zones have either been observed or inferred in the vicinity of the project area (Kumasi Landfill and Septage Facility General Operation and Maintenance Guidelines, January 2004).

An unpublished report by the operators of the facility (July 1999) indicates that the subsurface conditions were fairly uniform over the area and consisted of a relatively thin capping (typically 0.3 m) of organic topsoil, underlain by a mottled lateritic clay horizon which extended to depths of between 2.4 m and 3.6 m. Below the lateritic clay layer to the end of all boreholes was brownish red mottled stiff sandy clayey silt with mica flakes (completely weathered granite).

Figure 3.9 Picture of soil section at the study site.



**3.5 Field layout and data acquisition**

A topographical study of the area was undertaken to identify drainage pattern outside the perimeter of the landfill. An area lying on the south eastern part of the landfill boundary was selected for the survey (Fig. 3.9). As shown in the figure 3.1, the survey was conducted at both sides of the discharge stream. The area was chosen because it contains the discharge stream which leads all the waste water from the landfill to join the Oda River about 600 m away. At the time of the investigation the area was being used for small scale farming and sand winning. The study provides an ideal point to observe the effect of the landfilling and Septic waste treatment ponds on the surrounding environment.

Figure 3.10 Picture of study site showing discharge stream

Profiles of length 100 m were demarcated on both sides of the discharge stream (Fig. 3.10). These profiles run approximately perpendicular to the stream (in the east-west direction). The distance between adjacent profiles was 10 m. The distance between measurement points on each profile was 10 m. All the three intercoil spacing were used and data was for both the vertical and horizontal dipole mode in order to characterize the conductivity anomalies that may exist around the chosen site. The measurements were recorded in millisimens per meter ($mSm^{-1}$). At each station the horizontal dipole (HD) mode reading was taken first, followed by the vertical dipole (VD) mode, to probe different depths based on the respective intercoil spacing as shown in the table 3.1 below, derivation of these can be found at appendix B.

Table 3.1 Exploration depth for EM 34-3 at various intercoil spacings (McNeil, 1980)

| Intercoil Spacing (meters) | Exploration Depth | |
|---|---|---|
| | Horizontal Dipoles | Vertical Dipoles |
| 10 | 7.5 | 15 |
| 20 | 15 | 30 |
| 40 | 30 | 60 |

For the HD mode the receiver ($R_x$) and transmitter ($T_x$) coils were placed on the ground in such a way that their axes were parallel, but their planes were vertical and coplanar. The receiver coil was moved back and forth until the meter indicated a null setting and the terrain conductivity reading from a second digital meter and recorded (McNeil, 1980). Similarly, for the VD mode the coils were placed on the ground with their axes parallel, and coplanar. The procedures at each station were repeated until the desired total length of each traverse line was covered. Figure 3.11 below show the setting up and taking of measurements with the Geonics EM34-3 equipment on the field.



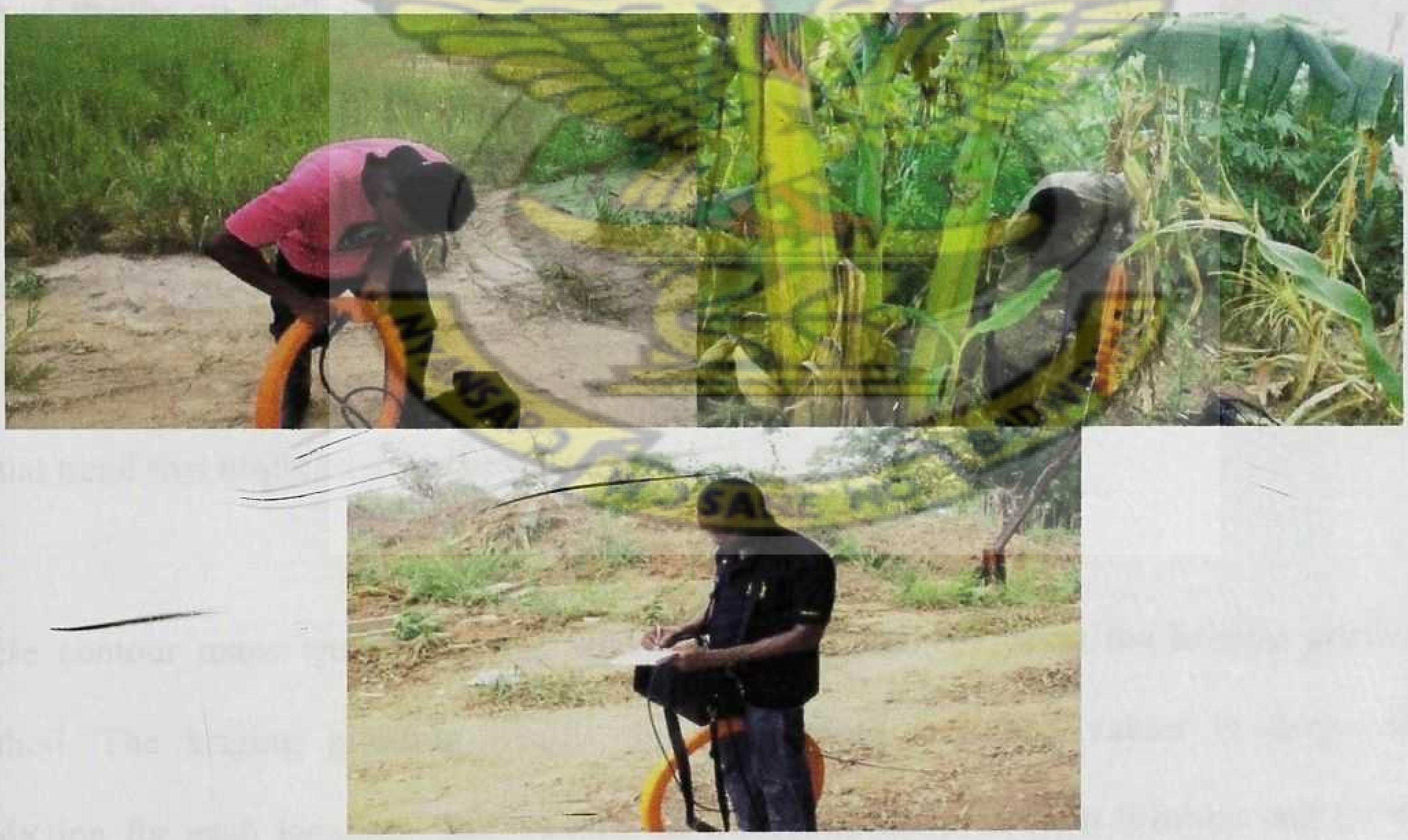

Figure 3.12 Setting up and taking measurements with the Geonics EM34-3 equipment

# CHAPTER FOUR

# RESULTS

## 4 .1 Introduction

The data was acquired along sixteen east – west profiles, each of length 100 m, and run approximately perpendicular to the discharge stream. There were seven and nine profiles respectively on the right and left sides of the discharge stream. The total area covered is approximately 1400 $m^2$. The distance between measurement points was 10 m and all three intercoil separations of 10 m, 20 m and 40 m were used. At each site six data points were obtained by making measurements in both the horizontal and vertical dipole modes with the three intercoil separations.



The data acquired therefore represents lateral variations in apparent EM conductivity at various depths on each side of the discharge stream. These nominal exploration depths as dictated by the selected frequencies and intercoil separations are 7.5 m, 15.0 m and 30.0 m respectively for the horizontal dipole mode. For the vertical dipole mode, the respective depths are 15.0 m, 30.0 m and 60.0 m. For each of these exploration depths, the EM field data are first represented in the form of conductivity contours to visually identify any significant spatial trend that might exist in the EM dataset.

These contour maps were generated with Surfer (Version 10) using the kriging gridding method. The kriging gridding weighs the surrounding measured values to derive the prediction for each location. The weights are based on the prediction location and on the overall special arrangement among the measured points (Geoff Bohling, 2005). The advanced colour scheme was adopted with custom colours. Ten colours (user defined) were assigned to the apparent conductivity range of values. Table 4.1 below shows the colour scheme with the corresponding apparent conductivity range. As defined in the colour scheme, areas of high of conductivity are shown in Red, while areas of low conductivity are in Yellow.

Table 4.1 Colour Scheme with apparent conductivity range

| Colour | Apparent Conductivity Range $\sigma$/mSm$^{-1}$ |
|---|---|
| Red | 90 – 100 |
| Magenta | 80 – 89 |
| Orange | 70 – 79 |
| Pink | 60 – 69 |
| Brown | 50 – 59 |
| Purple | 40 – 49 |
| Cyan | 30 – 39 |
| Blue | 20 – 29 |
| Green | 10 – 19 |
| Yellow | 0 – 9 |



## 4.2 2-D representation of results (Surfer conductivity maps)

### 4.2.1 Horizontal Dipole (HD)

In Fig. 4.1, lateral apparent conductivity variations are shown at the depth of 7.5 m from the ground surface. The contour interval is 2 mSm$^{-1}$. On both sides of the discharge stream, conductivity exhibits laterally uniform decrease away from the stream and this is more evident at the right side of the stream.

On the right of the discharge stream, Analysis on the data indicates that 56.52 % of the profile points had apparent terrain conductivity values in the range of 10 mS/m to 19 mS/m. The locations of these points are joined by green coloured contour lines.

On the left side of the discharge stream, apparent conductivity data recorded fell within six apparent conductivity ranges. This is indicated by the six different coloured contoured lines displayed on the map. Analysis on the data indicates that 65.66 % of the profile points had apparent terrain conductivity values in the range of 0 to 9 mS/m. The locations of survey points having value that fall within this range are displayed with yellow coloured contour lines.

Fig. 4.2 depicts lateral apparent conductivity distribution at 15.0 m from the ground surface. It also shows uniform and relatively low apparent conductivity measurements. On the right side of the stream apparent conductivity is predominantly in the range of 10 – 19 $mSm^{-1}$. Analysis of the data indicates that this range of values forms 97.14 % of the total number of data acquired. On the left side of the discharge stream, 50 m from the stream and on profile eight, there exists an apparent conductivity spike which has a maximum conductivity range of 90 -100 $mSm^{-1}$ and a minimum range of 10 -20 $mSm^{-1}$. The lateral coverage of this spike is about 20 m by 20 m. The predominant range of conductivity recorded on this side fell within 0 – 9 $mSm^{-1}$.

The apparent conductivity distribution at the exploration depth of 30.0 m measured with the 40 m coil spacing in the HD mode are shown by the contours in fig. 4.3. Apparent conductivity predominant on right side is in the range of 30 – 39 $mSm^{-1}$(cyan coloured contours). The relatively highest values of apparent conductivity measured on this side fell within the range of 80 - 89 $mSm^{-1}$. The points where these data were recorded are connected with a purple coloured contour line which is close to the land fill boundary.

On the left side of the discharge stream, the apparent conductivity data acquired fell within three different ranges of apparent conductivity values. The majority of data acquired fell within the 30 – 39 $mSm^{-1}$ range (cyan coloured contours). Followed by the 40 – 49 $mSm^{-1}$ range (purple coloured contours) and 50 – 59 $mSm^{-1}$ range (brown coloured contours).

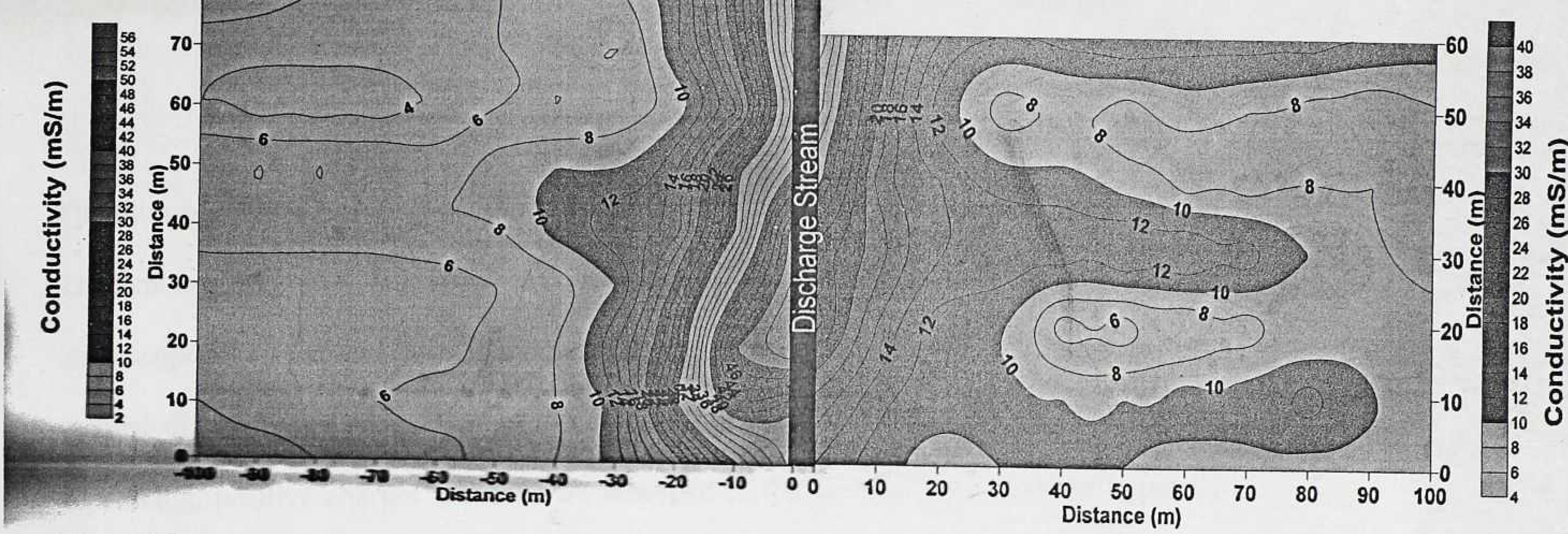


Figure 4.1 Contour maps of apparent terrain conductivity acquired with the EM34-3 instrument operated in Horizontal Dipole (HD) mode with coil separation of 10 m (exploration depth of 7.5 m).



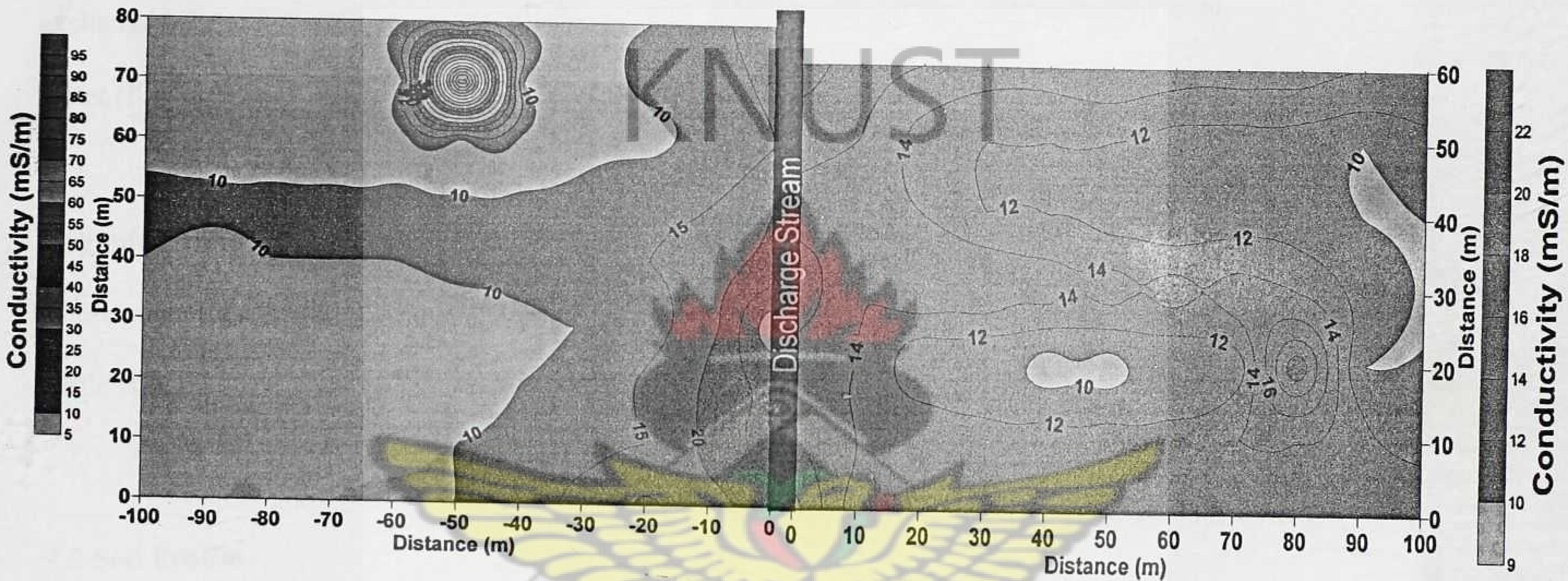


Figure 4.2 Contour maps of apparent terrain conductivity acquired with the EM34-3 instrument operated in Horizontal Dipole (HD) mode with coil separation of 20 m (exploration depth of 15 m).

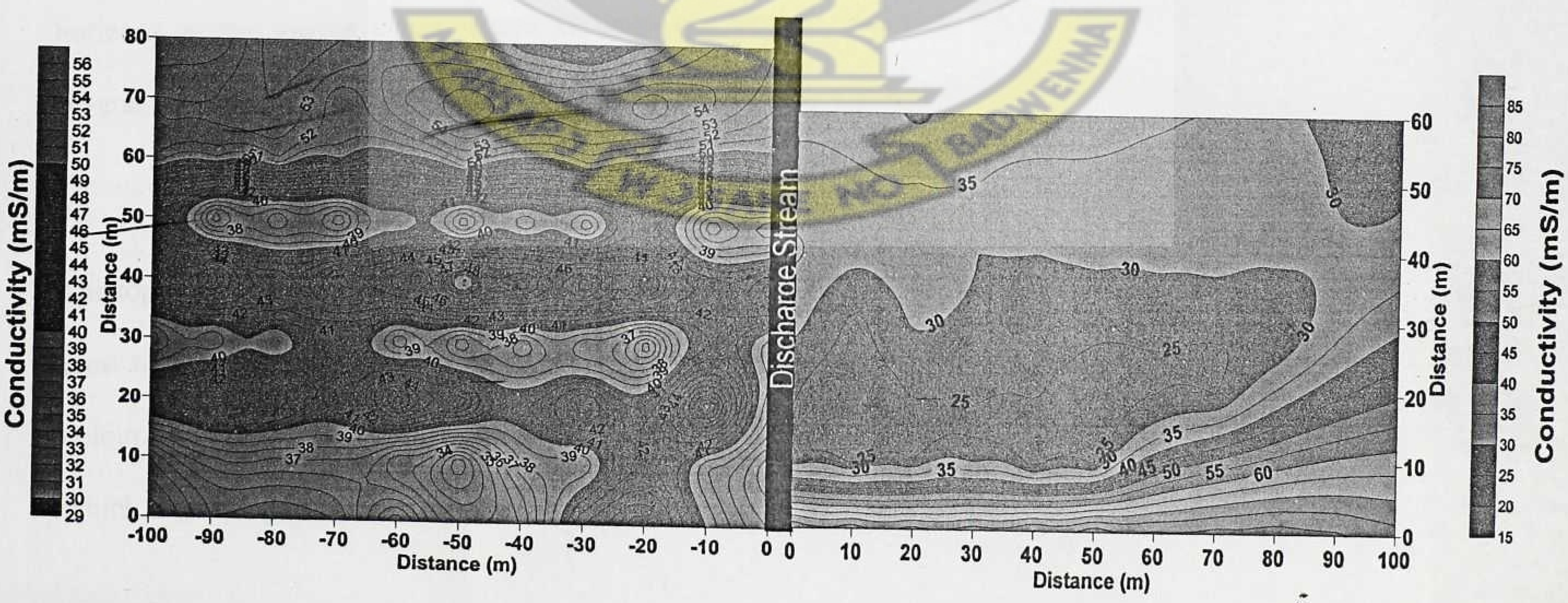


Figure 4.3 Contour maps of apparent terrain conductivity acquired with the EM34-3 instrument operated in Horizontal Dipole (HD) mode with coil separation of 40 m (exploration depth of 30 m).

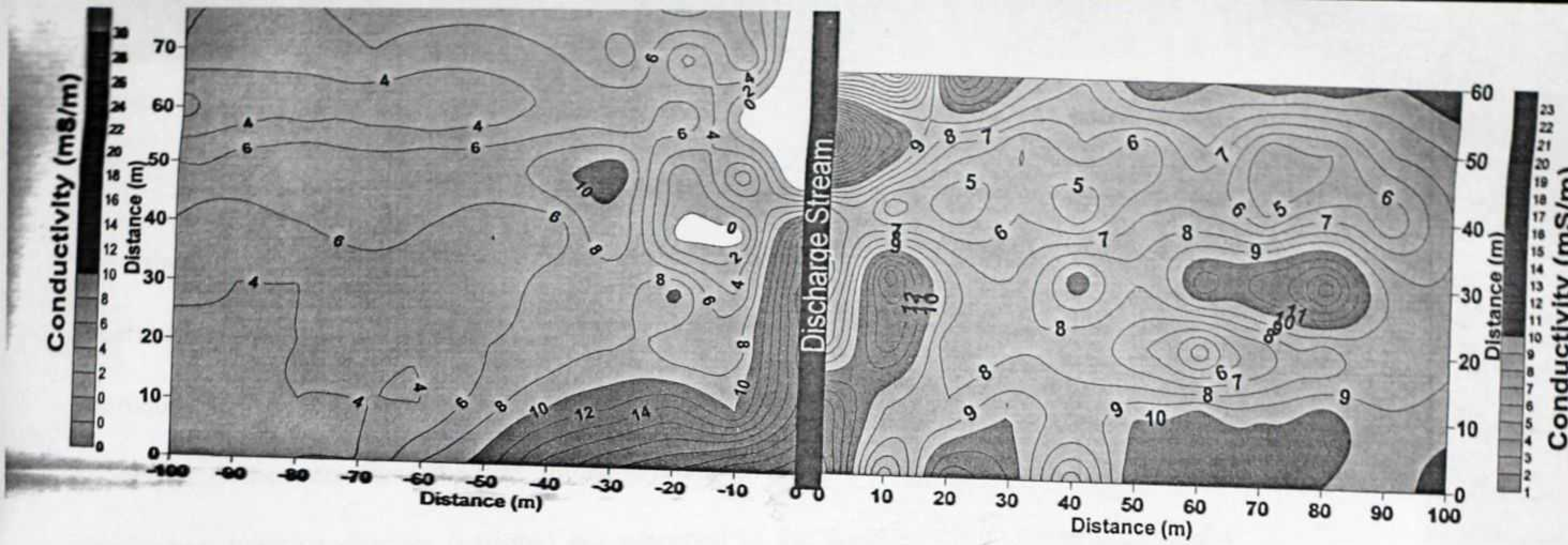


Figure 4.4 Contour maps of apparent terrain conductivity acquired with the EM34-3 instrument operated in Vertical Dipole (VD) mode with coil separation of 10 m (exploration depth of 15 m).



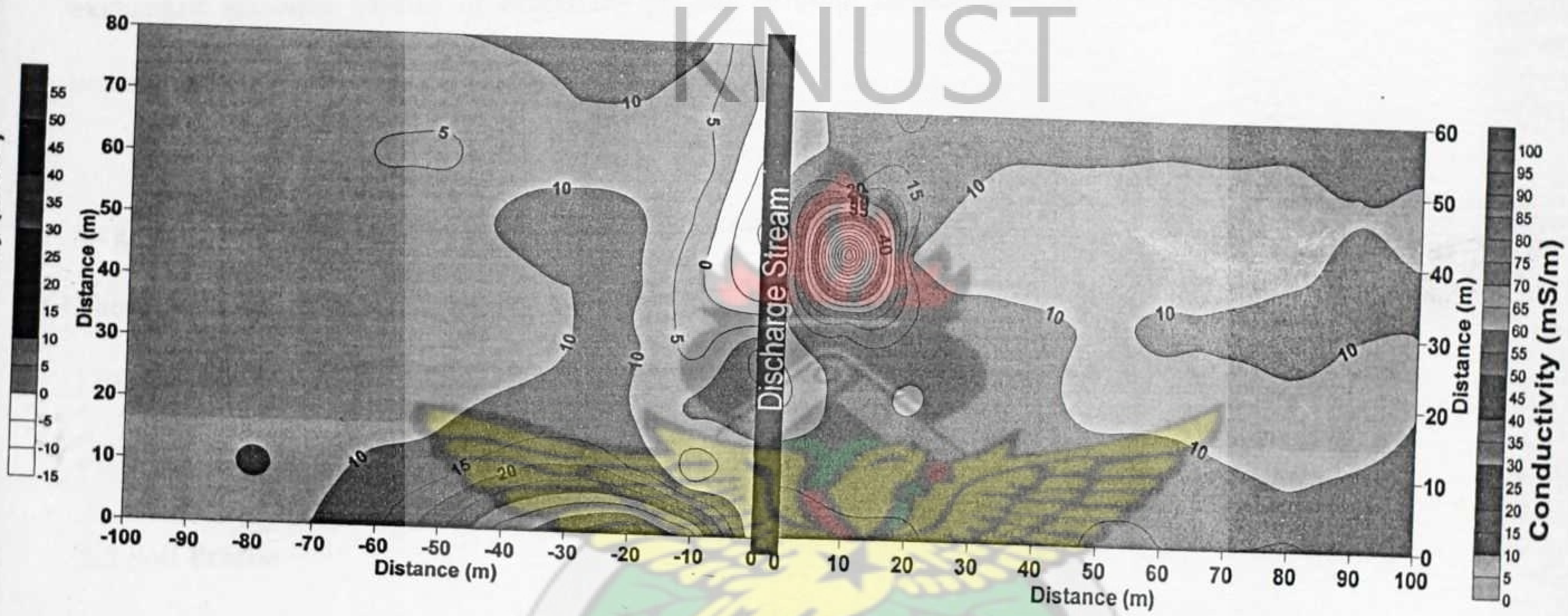


**Figure 4.5** **Contour maps of** apparent terrain conductivity acquired with the EM34-3 instrument operated in Vertical Dipole (VD) mode with coil separation of 20 m (exploration depth of 30 m).


Figure 4.6 Contour maps of apparent terrain conductivity acquired with the EM34-3 instrument operated in Vertical Dipole (VD) mode with coil separation of 20 m (exploration depth of 60 m).

### 4.2.2 Vertical Dipole (VD)

Figs 4.4 – 4.6 shows the contour for data acquired with the instrument operated in vertical dipole mode for the various intercoil spacings. They show the apparent conductivity at various depths on both sides of the discharge stream.

In Fig. 4.4, lateral apparent conductivity variations are shown at the depth of 15 m from the ground surface. Both sides of the discharge stream, had predominant conductivity values that fell within the range of 0 – 9 $mSm^{-1}$ (yellow coloured contour lines) White coloured contour lines which begins from profile 5 to 8 along the left side of the discharge stream account for apparent conductivity values that were negative. The highest conductivity values in the range of 20 – 29 $mSm^{-1}$ exists at a relatively small portion of the study area close to the landfill boundary.

Fig. 4.5 depicts lateral apparent conductivity distribution at 30.0 m from the ground surface. The right side of the discharge stream has a predominant conductivity value that falls within the range of 10 – 20 $mSm^{-1}$(green shades of contour lines). 10 m from the stream and on profile five, there exists an apparent conductivity spike which has a maximum conductivity range of 90 -100 $mSm^{-1}$ and a minimum range of 10 -20 $mSm^{-1}$. The lateral coverage of this spike is about 20 m by 20 m.

The predominant conductivity range on the left side of the discharge stream falls within the 0 – 10 $mSm^{-1}$(yellow shades of contour lines). The highest conductivity values in the range of 50 – 59 $mSm^{-1}$ exist at points close to the landfill boundary and 10 m from the discharge stream. The range decreases gradually to within 10 -19 $mSm^{-1}$ as data points are sampled from profile 1 to 10. White coloured contour line which begins from profile 4 to 8 along the right side of the discharge stream account for apparent conductivity data that that were negative.

The apparent conductivity distribution at the exploration depth of 60.0 m measured with the 40 m coil spacing in the VD mode are shown by the contours in fig. 4.6. The predominant values recorded on the right side of the discharge stream fell within the range of 20 – 29 $mSm^{-1}$(blue shaded contours). On this side, a relatively high conductivity valùe in the range of 90 – 100 $mSm^{-1}$ exists along points close to the landfill boundary. This range of values gradually decrease to 30 – 40 $mSm^{-1}$ towards profile line 3.

Two dominant apparent conductivity values were recorded on the left side of the discharge stream. They fall within range 30 – 39 $mSm^{-1}$(cyan shaded contours) and 50 – 59 $mSm^{-1}$ (brown shades contours) respectively. On this side, a relatively high conductivity value in the range of 90 – 100 $mSm^{-1}$ exists at a point 20 m from the discharge stream along profile 0 (landfill Boundary). This range of values gradually decreases to 40 – 49 $mSm^{-1}$ towards profile line 10

### 4.3 1-D Frequency Domain EM Modeling

#### 4.3.1 Preamble

Attempts have also been made to explore the characteristics of the overburden. The overburden is important because it serves to reduce or eliminate the transport of contaminants into the aquifer system. The subsurface under this study area is modelled as a two layer conductivity structure representing top protective overburden and the variably fractured bedrock.

Resolving the two-layered earth is accomplished by varying the inter coil separation and using the EM 34-3 equipment in both the vertical and the horizontal dipole modes at a particular measuring point. Thus by expanding the intercoil spacing and also using the two dipole modes, vertical conductivity variation is achieved.



To invert Data, – the Marquardt-Levenberg or damped least-squares method (Lines and Treitel 1984) is applied to automatically adjust the model thickness and conductivity to reduce the different between the calculated and measured apparent conductivity values. The nonlinear model calculation method which uses the digital filter method (Koefoed et al. 1972, Guptasarma and Singh, 1997) and gives significantly more accurate results for moderate high conductivity values was applied. Since the calculation time for 1-D model is very short, for most data set, it is preferable to use the nonlinear method.



### 4.3.2 Representation of the 1-D modeling

At each observation point on a profile, a 1-D six conductivity measurements are made reflecting effects from subsurface layers at different depths. The FreqEM programme admits these measurements including the coil configuration, frequency corresponding to the intercoil separation, the maximum number of layers as input parameters. The programme iterates to generate a two layer conductivity model for that point. A measure of the goodness of fit determined by the rms error is also computed. This is repeated for all the points on the profile and also for all the profiles. Without the benefit of going further to use a 2-D or 3-D application package, average layer parameters consisting of the bulk conductivities of the top and bottom layers, and the thickness of the substratum are computed using the Surfer (10). The results indicating the situation pertaining to the left side of the discharge stream are shown in Figures 4.7, 4.8 and 4.9 below.

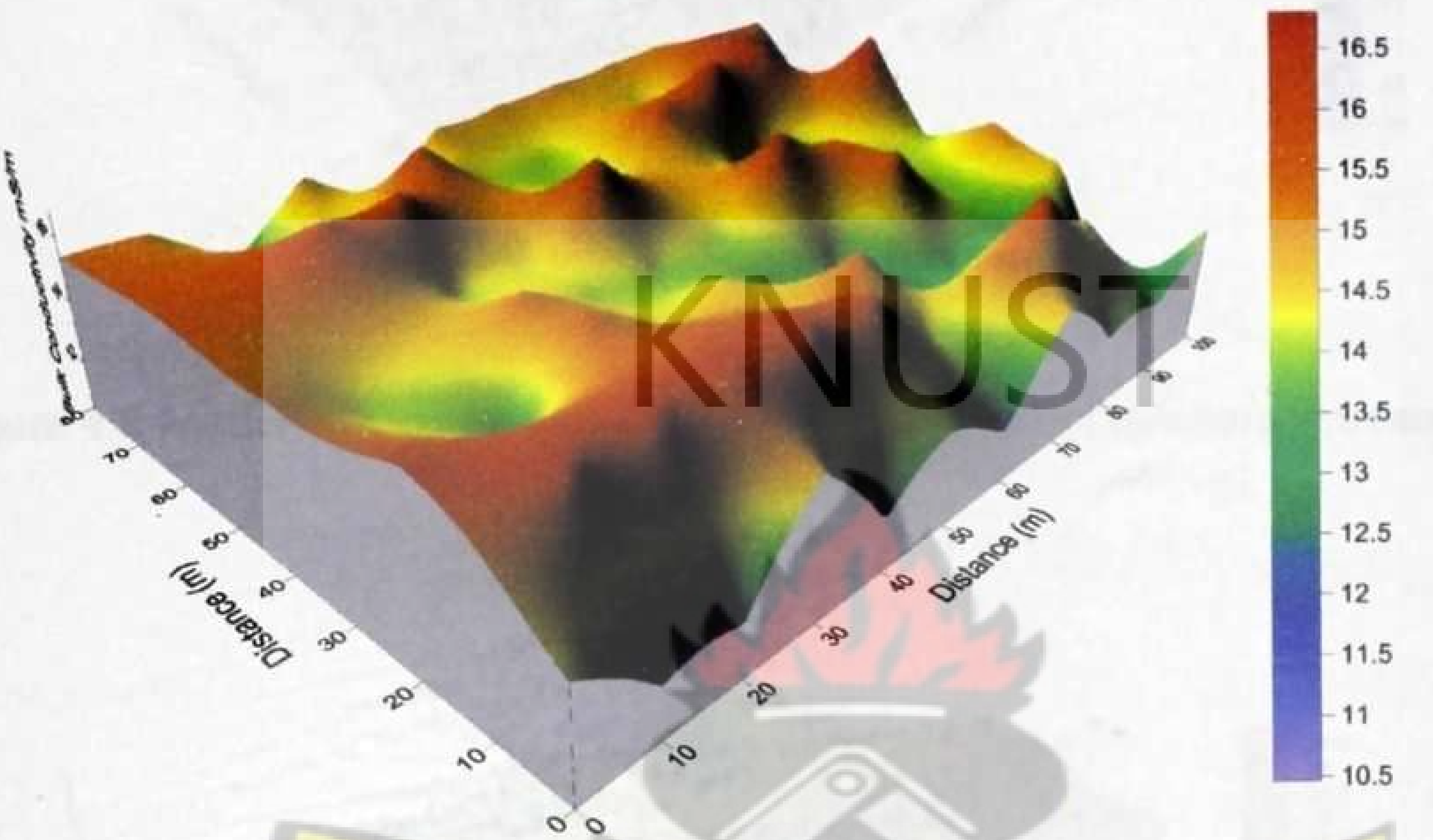




Figure 4.7 Modeled Conductivity of top layer (left of discharge stream)

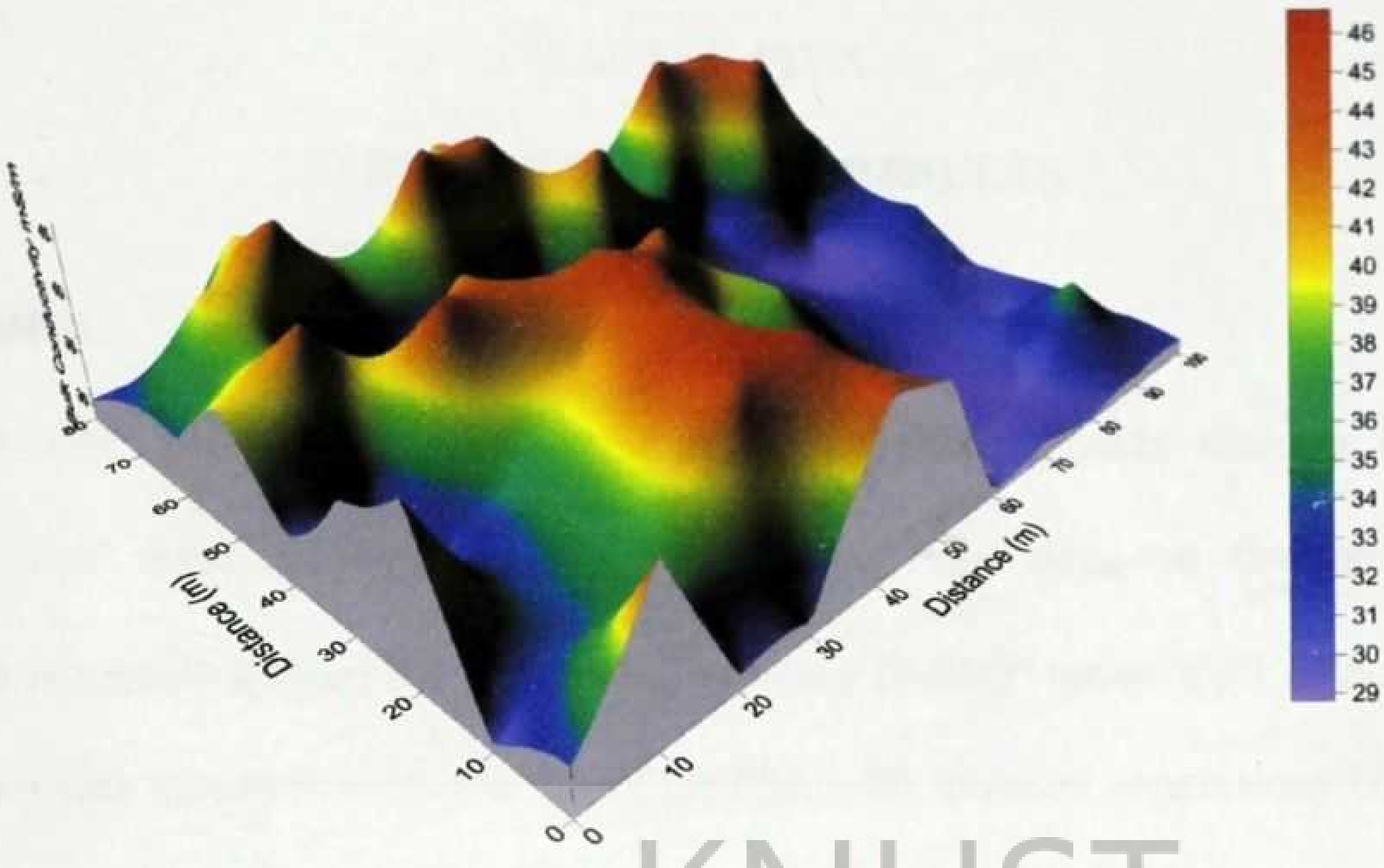


Figure 4.8 Modelled Conductivity of bottom layer (left of discharge stream)

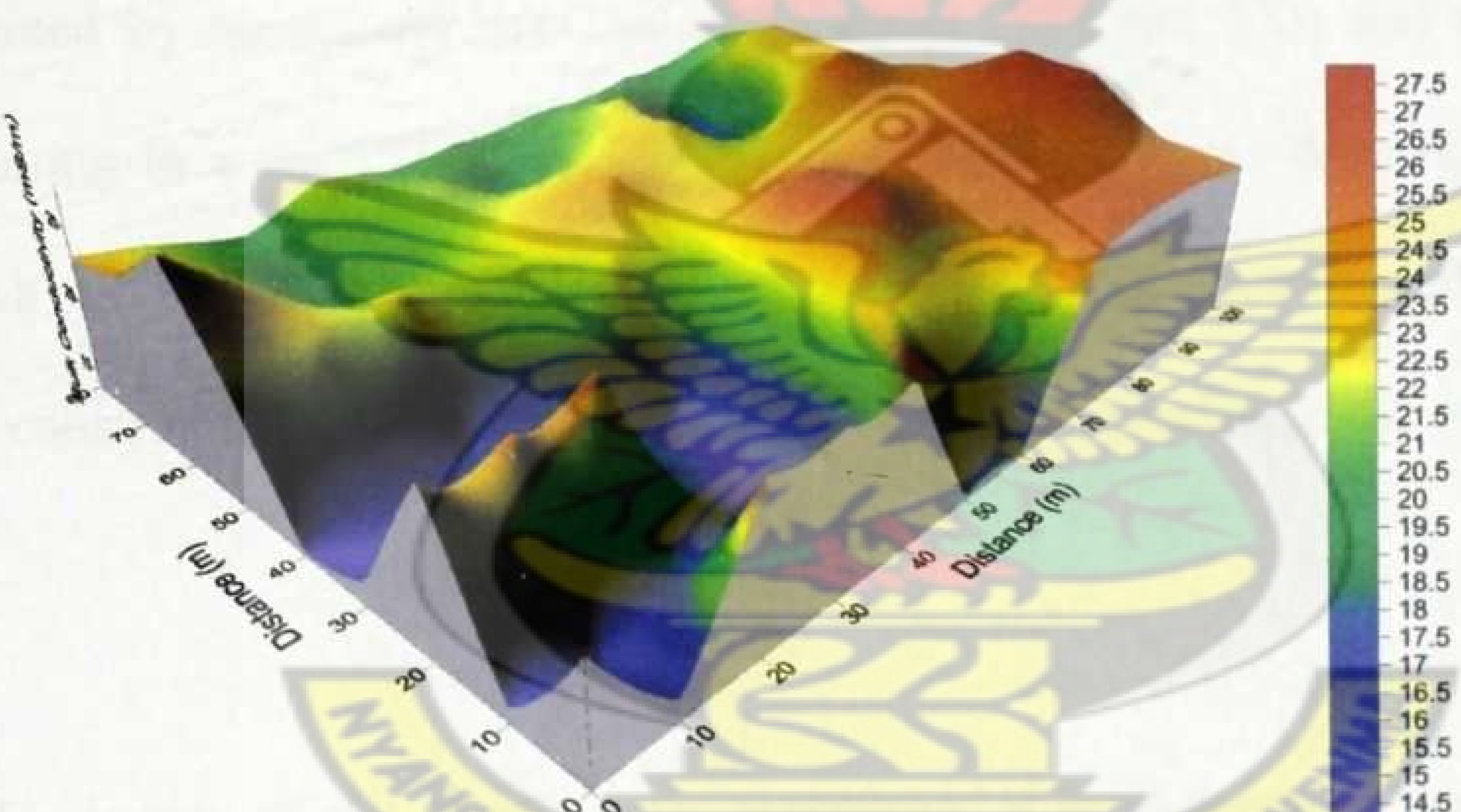


Figure 4.9 Modelled thickness of top layer (left of Discharge stream)

# CHAPTER FIVE

# INTERPRETATION OF RESULTS

## 5.1 Introduction

The Geonics EM 34-3, like all terrain conductivity meters reads directly in apparent conductivity and most surveys using the instrument are done in the profile mode, interpretation is usually qualitative and of the "anomaly finding" nature (US EPA, 2011). The area of interest was surveyed with a series of profiles with intercoil separations 10, 20 and 40 m and station spacing of 10 m to produce a 2-dimensional map of apparent conductivity. In this research, therefore, interpretation is first done based upon the lateral distribution of apparent conductivity. Secondly, limited information about the variation of conductivity with depth was obtained by measuring two coil orientations (HD and VD) and three intercoil separations resulting in a maximum of six observations at a station. With this, geoelectric parameters, such as layer thicknesses and conductivities, were determined and without admitting other constraints, a two-layer model was chosen to characterize the overburden and the substratum.

In discussing the causes of the conductivity anomalies, it is understood that non-organic (ionic) groundwater or soil contamination usually results in an increase in the conductivity of the soil or groundwater. For example, in a sandy soil, the addition of 25 ppm of ionic material to groundwater increases ground conductivity by approximately 1 mS/m (US EPA, 2011). The interpretational problem is to explain the changes in conductivity besides the conductivity variations caused by other parameters such as changing lithology. But lithologic variations are not considered potential interference factor at this site.

Organic contaminants are generally insulators and thus tend to reduce the ground conductivity, although with much less effect than an equivalent percentage of ionic contaminant. Fortunately, in many cases where organic substances are present, there are ionic materials as well, and the plume is mapped on the theory that the spatial distribution of both organic and ionic substances is essentially the same.

Two surfaces are shown on each figure - two orientations (VD and HD) for every particular separation. In the discussions, premium is placed on anomalies which repeat for the two coil configurations; otherwise such anomalies could be skipped and attributed to measurement uncertainty or some other disturbance.

Conductivity is linked to salinity, and soluble salts are more likely to build up in areas where there is less direct communication with surface water, areas of higher conductivity could be interpreted as areas with more confined systems, whereas areas with lower conductivity could be interpreted as zones with greater surface-water and groundwater interaction.

Conductivity variation is also linked to the soil moisture variations that themselves are related to the valley slope and other topographic undulations. Substantial topographic variations may affect the EM readings such that an increase in elevation will correspond to a decrease in conductivity (Duran, 1984). Changes in topography can often be correlated with changes in the depth to ground water. The topographic variations within the survey site is however minimal and considered to have no appreciable effect on the EM data.

Cultural effects are also minimal because no pipes or power lines were closed to the survey site, except the landfill perimeter fencing.

In summary, the effects of cultural and natural interferences on the geophysical data collected at the site are interpreted to be minimal. Therefore, anomalies and trends identified in the data can most likely be attributed to electrolytic solutions and or elevated concentrations of ionic contaminants from the leachates.



**5.2 Lateral Apparent Conductivity Distribution**

The geophysical data collected with Geonics EM 34-3 survey have been contoured to represent the terrain conductivity in $mSm^{-1}$ (Figures 4.1 – 4.6). The measured conductivity maps for the horizontal and vertical coils are respectively shown in Figs 5.1 and 5.2 where, here emphasis has been placed on the relative exploration depths of the three intercoil separations. The background conductivity which is a reflection of some sort of an average conductivity at the optimum depths on both sides of the discharge stream are shown in Tables 5.1 and 5.2.

A comparison of the background conductivities of the top layers indicates one major anomalous zone (A1), at the left side of the discharge stream (Fig. 5.1, top layer). With a background conductivity range of 12.3 – 13.1 $mSm^{-1}$, as indicated by the horizontal dipole configuration, this anomalous zone has a conductivity range of 40.0 – 60.0 $mSm^{-1}$. Since this anomaly is not entirely corroborated by the VD measurements (Fig. 5.2 top layer), which portrays more uniform terrain conductivity, it implies the anomaly is a reflection of more shallow effects. It probably reflects the conductivity of the water, with possibly higher ionic content, within that marshy part of the site.

Table 5.1 Summary of the background conductivities on the right side of discharge stream

| Coil Separation (m) | Depth (m) | Dipole | No. of Readings | Min ($mSm^{-1}$) | Max ($mSm^{-1}$) | Average ($mSm^{-1}$) |
|---|---|---|---|---|---|---|
| 10 | 7.5 | HD | 69 | 5 | 38 | 12.3 |
| 10 | 15 | VD | 69 | 1 | 23 | 8.6 |
| 20 | 15 | HD | 72 | 9 | 22 | 13.4 |
| 20 | 30 | VD | 72 | 3 | 99 | 12.4 |
| 40 | 30 | HD | 65 | 22 | 84 | 38.0 |
| 40 | 60 | VD | 65 | 21 | 92 | 37.6 |



Table 5.2 Summary of the background conductivities on the left side of discharge stream

| Coil Separation (m) | Depth m | Dipole | No. of Readings | Min ($mSm^{-1}$) | Max ($mSm^{-1}$) | Average ($mSm^{-1}$) |
|---|---|---|---|---|---|---|
| 10 | 7.5 | HD | 99 | 3 | 54 | 13.1 |
| 10 | 15 | VD | 99 | -7 | 28 | 6.7 |
| 20 | 15 | HD | 98 | 6 | 98 | 12.4 |
| 20 | 30 | VD | 99 | -11 | 52 | 9.7 |
| 40 | 30 | HD | 98 | 30 | 56 | 43.7 |
| 40 | 60 | VD | 99 | 19 | 100 | 44.9 |

Moving down further to the depths explored by the 20 m coil separation, measurements by both coil configurations show substantially uniform conductivity subsurface layer. On both sides of the discharge stream, the background conductivities are almost the same (13.4 and 12.4 $mSm^{-1}$respectively). There are however, two anomalous zones of discrete nature, SP1(Fig. 5.1 middle layer) and SP2 (Fig. 5.2 middle layer) at the left and right sides respectively. SP1 is a high conductivity spike located 50 m from the discharge stream on profile eight. It possesses a maximum conductivity within the range 90 – 100 $mSm^{-1}$. Similarly, there is a high conductivity spike SP2 also of maximum conductivity within range of 90 – 100 $mSm^{-1}$ located 10 m from the discharge stream on profile 5 on the right side.

These spikes could be due to a buried high conductivity material, like metal. They are more likely to be statistical outliers or measurements errors. They can therefore be discharged from being a possible contaminant plume.

The (Table 5.3) below summarizes the modeled layer parameters of the 1-D modeling. It indicates the bulk or formation conductivities and thickness of the top layer. The top layer has average conductivity less than the half-space. This might be due to the fact that the top surface materials have more interaction with water thereby diluting any possible contaminant build up. The half space being more conductive might also indicate that it does not constitute the fresh bedrock.

Table 5.3 Modelled layer parameters from the FreqEM software.

| **Layer Parameter** | **Left of discharge stream** | | | **Right of discharge stream** | | |
|---|---|---|---|---|---|---|
| | **Ave** | **Min** | **Max** | **Ave** | **Min** | **Max** |
| Mean conductivity of top layer $\sigma_1$/mSm$^{-1}$ | **14.68** | 12.05 | 16.93 | **15.32** | 12.80 | 19.1 |
| Mean conductivity of bottom layer $\sigma_2$/mSm$^{-1}$ | **34.46** | 29.21 | 41.3 | **40.15** | 34.2 | 46.2 |
| Thickness of top layer $h_1$/m | **21.42** | 14.00 | 28.00 | **18.73** | 13.83 | 24.5 |

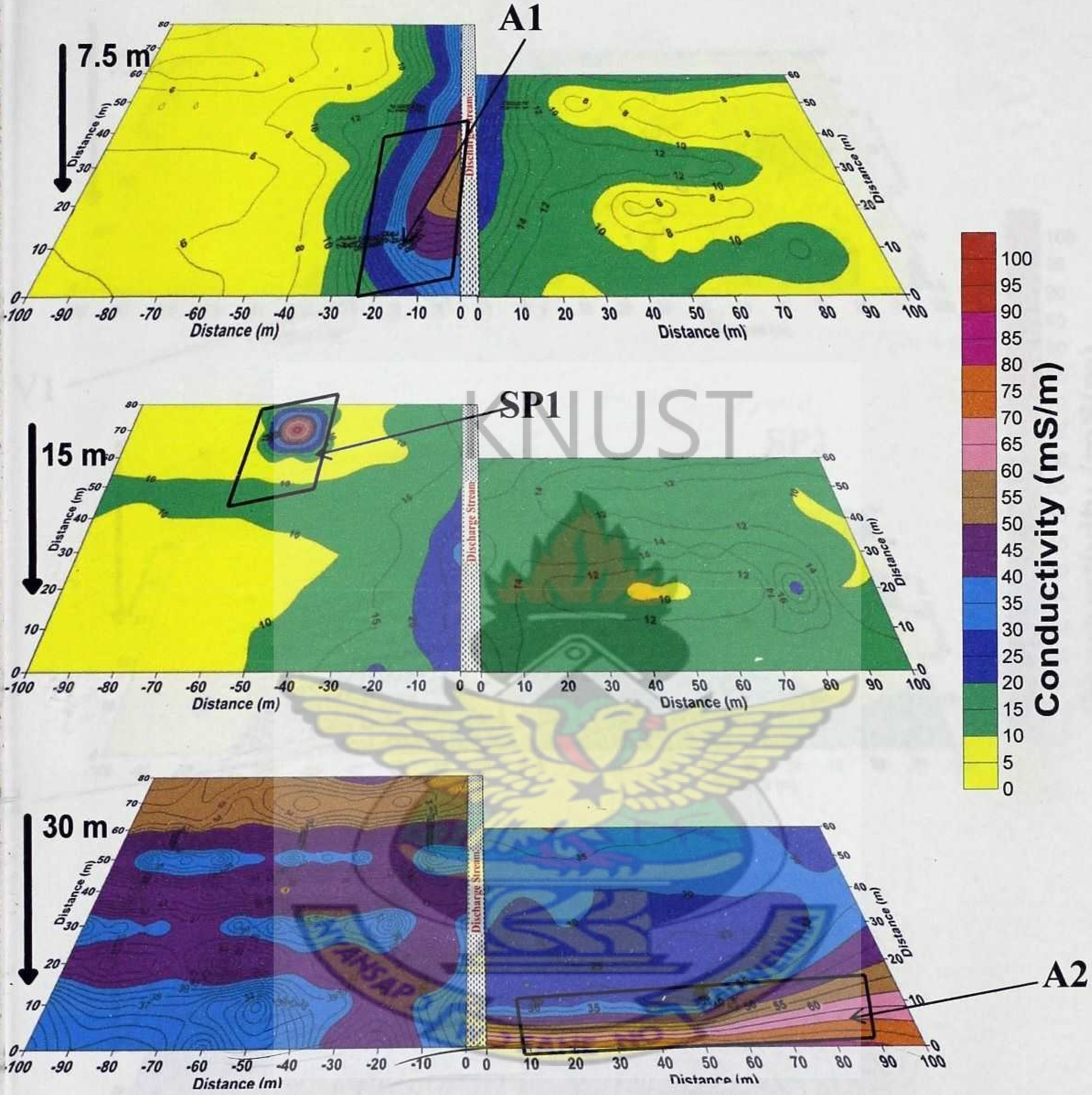


Figure 5.1Contour maps of apparent terrain conductivity acquired with the EM34-3 instrument operated in Horizontal Dipole (HD) mode with coil separation of 10 m, 20 m and 40 m and corresponding depth of 7.5 m 15 m and 30 m respectfully.

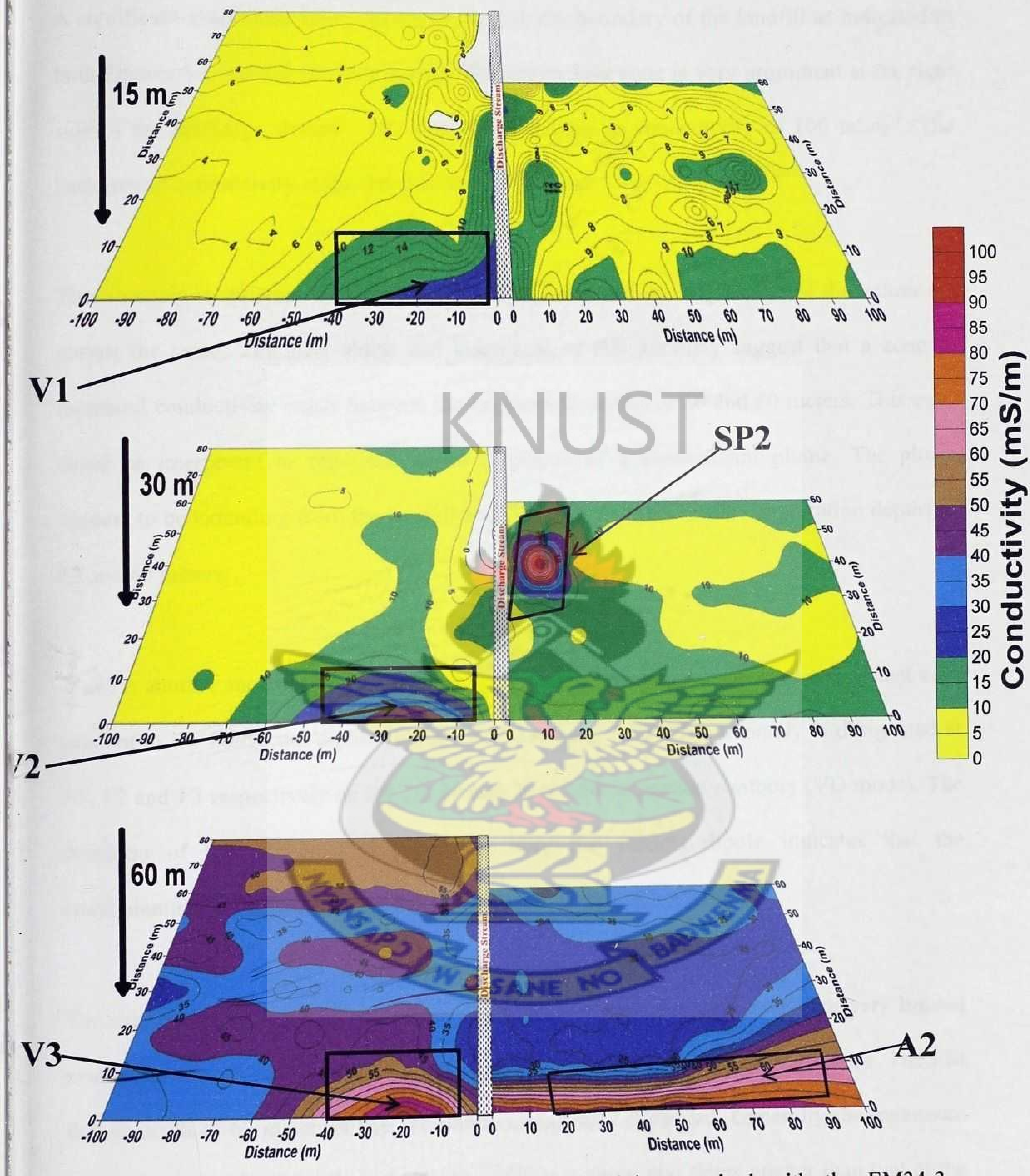




Figure 5.2 Contour maps of apparent terrain conductivity acquired with the EM34-3 instrument operated in Vertical Dipole (VD) mode with coil separation of 10 m, 20 m and 40 m and corresponding depth of 7.5 m 15 m and 30 m respectfully.

A significant anomalous zone, A2 exists close to the boundary of the landfill as indicated in both Figures 5.1 and 5.2 (bottom layers). This anomalous zone is very prominent at the right side of the discharge stream. The zone has a maximum conductivity of 100 $mSm^{-1}$. The background conductivity at this level is within the range 37.6 – 44.9 $mSm^{-1}$.

This anomaly is apparent in both dipole configurations and the magnitudes of the values are almost the same. The size, shape and magnitude of this anomaly suggest that a zone of increased conductivity exists between the exploration depths of 30 and 60 meters. This zone could be interpreted to represent lateral migration of a contaminant plume. The plume appears to be extending from the landfill and concentrated between the exploration depths of 30 and 60 meters.

There is another anomaly that is apparent in the vertical dipole configuration and almost non-existent in the horizontal dipole (Figures 4.3 – 4.6 and 5.2b). The anomaly is designated at *V*1, *V*2 and *V*3 respectively on the 10, 20 and 30 m coil separation contours (VD mode). The detection of this contaminant plume by only the vertical dipole indicates that the contamination is within a vertical dike-like feature (Boniwell, 1987).

The exploration depth of 15 m, the EM 34 – 3 indicates a small plume (*V*1) of very limited extent. At an exploration depth of 30 m, the plume increases in size and magnitude. The EM data at depth of 60 m shows that the plume has slightly expanded. Generally the maximum conductivity of this anomaly at the depth of 60 m is about two times greater than that at the 30 m depth and a little greater than three times the maximum conductivity at 15 m. The doubling of conductivity between 30 to 60 m in depth, coupled with only a slight expansion in size of the plume, suggest vertical migration of contaminants within a probably fault zone or some form of vertical structural weakness.

From the results of the 1-D modelling, the overburden in major part of the surveyed area is quite thick. Its thickness is within the range of 13.83 – 24.50 m, with mean depths of 21.42 m and 18.73 m on the left and right side of the discharge stream respectively. The bulk conductivity of the top layer is within the range of 12.05 – 19.10 $mSm^{-1}$, with mean conductivities 14.68 $mSm^{-1}$and 15.32 $mSm^{-1}$ of the left and right sides of the discharge stream respectively. The second layer representing the substratum has bulk conductivity in the range of 29 .21 – 46.2 $mSm^{-1}$. The mean conductivities are 34.46 and 40.15 $mSm^{-1}$ of the left and right sides of the discharge stream respectively.

## CHAPTER SIX

## CONCLUSIONS AND RECOMMENDATIONS

### 6.1 Conclusions

Electromagnetic profiling has been carried out on a section of the lands contiguous to the Dompoase landfill facility, Kumasi, to outline possible conductive layers probably connected with leachate communication. The objectives of the survey basically amounted to examining two hypotheses; that contaminant plumes are migrating laterally away from the discharge stream and from the landfill, and also that the contaminant plumes are seeping down into the groundwater aquifer system. The study was based solely on practical field survey with the terrain electromagnetic equipment – Geonics EM 34-3.



The high conductivity found within the depths 30 to 60 m close to the southern boundary of the landfill might suggest leachate communication from the landfill. The linear pattern of the contour lines in that anomalous zone probably indicate the presence of zones of weakness trending approximately perpendicular to the direction of flow of the discharge stream. This weak zone could account for the lateral spread of leachate within those depths, where leachate plume has so far migrated about 30 m from the landfill southern boundary.

The discharge stream carries waste water from the septic and leachate treatment ponds. Anomalously high ionic contaminants escaping into the stream will be a reflection on the level of efficiency of the treatment process. The research does not indicate that any such anomalously high volumes of ionic contaminants are getting into the discharge stream. This is evident on the lack of any significantly high anomalous conductivity zones close to the discharge stream at the surface and at depths.

A major implication of these conclusions is in terms of aquifer protection. In terms of aquifer protection it must be noted that the aquifer in the adjoining land is considerably well protected. The overburden in major part of the surveyed area is quite thick. Its thickness is within the range of 13.83 – 24.50 m, with mean depths of 21.42 m and 18.73 m on the left and right side of the discharge stream respectively. The bulk conductivity of the top layer is within the range of 12.05 – 19.10 $mSm^{-1}$, with mean conductivities 14.68 $mSm^{-1}$and 15.32 $mSm^{-1}$ of the left and right sides of the discharge stream respectively. The second layer representing the substratum has bulk conductivity in the range of 22 – 47 $mSm^{-1}$. The mean conductivities are 34.46 and 40.15 $mSm^{-1}$ of the left and right sides of the discharge stream respectively.



### 6.2 Recommendations

The terrain conductivity technique, used in such environmental studies, offers the benefits of user-friendly instrumentation, rapid data collection, and is completely non-invasive. Though the results of this research do not suggest any eminent threat to the aquifer system by leachate communication from the landfill facility, with the above advantages of the equipment and procedure, periodic repetitions of this procedure would be appropriate. This repetition could be in the form of electrical conductivity tomography, to produce a time-lapse 4D electrical conductivity monitoring. This is a technique for providing depth, volumetric, and time dependent imaging of subsurface lecheate communication. This technique has broad applications for planning potential remediation programs even after the facility has exhausted its working life.

# REFERENCES

Acworth, R., 2006, Integration of multi-channel piezometry and electrical tomography to better define chemical heterogeneity in a landfill leachate plume within a sand acquifer. *Journal of Contaminant Hydrology, 83*, 2-4.

Akiti, T.T., 1982, "Nitrate levels in some granitic aquifers from Ghana. Published at the International Symposium on "impact of Agricultural Activities on Groundwater, " Prague, Czechoslovakia.

Alwail T.A., 1996, Mapping of Shallow Karstic Aquifers by Electromagnetic Method. Sageep. , pp. 1055.

Aziz, H. A., Alias, S., Adlan, M. N., Faridah, Asaari, A. H. and Zahari, M. S., 2007, 'Colour removal from landfill leachate by coagulation and flocculation processes', Bioresource Technology, vol. 98, no. 1, pp. 218-220.

Babu, H. V. R., Rao, N. K. and Kumar, V. V., 1991, Bedrock topography from magnetic anomalies - An aid for groundwater exploration in hard-rock terrains (short note): Geophysics, 56, no. 07, 1051 -1054.

Barker, J. F., Acton, D. W., 1992, 'In situ biodegradation potential of aromatic hydrocarbons in anaerobic groundwaters', Journal of Contaminant Hydrology, vol. 9, no. 4, pp. 325-352.

Barker, R. D., 1990, Investigation of groundwater salinity by geophysical methods, in Ward, S. H., Ed., Geotechnical and environmental geophysics: Society of Exploration Geophysicists, 201 - 211.

Bastianon, D., Matos, B. A., Aquino, W. F., Pacheco, A. and Mendes, J. M. B., 2000,. Geophysical surveying to investigate groundwater contamination by a cemetery. The

Annual Meeting of the Environmental and Engineering Geophysical Society. Arlington. 709-718.

Beeson, S. and Jones, C.R.C., 1988, The Combined EMT/VES Geophysical Method for Siting Boreholes. Ground Water 26:54-63.

Benson, C. H. and Othman, M. A., 1993, 'Hydraulic and Mechanical Characteristics of a Compacted Municipal Solid Waste Compost', Waste Management & Research, vol. 11, no. 2, pp. 127-142.

Bjerg, P. L., Albrechtsen, H. J., Kjeldsen, P., Christensen, T. H., Cozzarelli, I. M. and Heinrich, D. H., 2003, 'The Groundwater Geochemistry of Waste Disposal Facilities', in (ed.), Treatise on Geochemistry, Pergamon, Oxford, pp. 579-612.

Boniwell, S., 1987, Geonics Limited, Sensitivities of the Horizontal and vertical Dipoles of the EM Terrain conductivity.

Bouazza, A. and Impe, W. F. V., 1998, 'Liner design for waste disposal sites', Environmental Geology, vol. V35, no. 1, pp. 41-54.

Bowling, S.D., Schultz, D.D. and Wolt, W.E., 1997, A geophysical and geostatistical method for evaluating potential surface contamination from feedlot retention ponds. ASAE Paper no. 972087. ASAE, St. Joseph, MI. 20 p.

Brune, D.E., and Doolittle, J.A., 1990, Locating lagoon seepage with radar and electromagnetic survey. Environ. Geol. Water Sci. 16:195–207.

Carruthers, R. M. and Smith, I. F., 1992, The Use of Ground Electrical Methods for Siting Water Supply Boreholes in Shallow Crystalline Basement Terrains. In: E. P. Wight and W. G. Burgess, (eds), The Hydrogeology of Crystalline Basement Aquifers in Africa. Geological Society Special Publication, No. 66, p. 203 -220.

Christensen, T. H., Kjeldsen, P., Albrechtsen, H. J., Heron, G., Nielsen, P. H., Bjerg, P. L. and Holm, P. E., 1994, 'Attenuation of Landfill Leachate Pollutants in Aquifers', Critical Reviews in Environmental Science and Technology, vol. 24, no. 2, pp. 119-202.

Christensen, T. H., Kjeldsen, P., Bjerg, P. L., Jensen, D. L., Christensen, J. B., Baun, A., Albrechtsen, H. J. and Heron, G., 2001, 'Biogeochemistry of landfill leachate plumes', Applied Geochemistry, vol. 16, no. 7-8, pp. 659-718.

Chofqi, A., Younsi, A., Lhadi, E. K., Mania, J., Mudry, J. and Veron, A., 2004, 'Environmental impact of an urban landfill on a coastal aquifer (El Jadida, Morocco)', Journal of African Earth Sciences, vol. 39, no. 3-5, pp. 509-516.

Cosgrave, T.M., Greenhouse, J.P. and Barker, J.F., 1987, Shallow Stratigraphic Reflections from Ground Penetrating Radar. In: Proc. 1st Nat. Outdoor Action Conf. on Aquifer Restoration, Ground Water Monitoring and Geophysical Methods, National Water Well Association, Dublin, OH, pp. 555-569.

Davis, S. N. and de Eiest, R. J. M., 1966, Ghyben-Herzberg Hydrostatic Conditions. Hydro geology, v. pp.238 - 239.

Doherty, L.H., 1963, "Electrical Conductivity of the Great Lakes", J.Res. Natl. Bur. Stds. (67D), pp 765 – 771

Drommerhausen, D.J., Radcliffe, D.E. Brune, D.E. and Gunter, H.D., 1995, Electromagnetic conductivity survey of dairies for groundwater nitrate. J. Environ. Qual. 24:1083–1091.

Duah A.A, 2006, "Groundwater Contamination in Ghana", CSIR Water Research Institute, Accra, Ghana.

Duran. P. B., 1984, The Effects of Cultural and Natural Interference on Electromagnetic Conductivity Data. Proceedings of the National Water Well Association/US Environmental Protection Agency Conference on Surface and Borehole Geophysical Methods in Groundwater, NWWA, p. 509.

Eigenberg, R.A. and Nienaber, J.A., 1998, Electromagnetic survey of cornfield with repeated manure applications. J. Environ. Qual. 27:1511–1515.

Eigenberg, R.A., Korthals, R.L. and Nienaber, J.A., 1998, Geophysical electromagnetic survey methods applied to agricultural waste sites. J. Environ. Qual. 27:215–219.

El-Fadel, M., Bou-Zeid, E., Chahine, W. and Alayli, B., 2002, 'Temporal variation of leachate quality from pre-sorted and baled municipal solid waste with high organic and moisture content', Waste Management, vol. 22, no. 3, pp. 269-282.

Fawcett, J. D., 1989, Hydrogeologic assessment, design and remediation of a shallow groundwater contaminated zone. In, Proceedings of the Third National Outdoor Action Conference on Aquifer Restoration, Ground Water Monitoring and Geophysical Methods. Pp. 591-605. National Water Well Association, Orlando.

Freeze, R. A. and Cherry, J. A., 1979, Groundwater, Prentice-Hall Inc., London.

Geoff Bohling, 2005, Introduction to Geostatistics and Variogram Analysis. C&Pe 940.

Godio, A., Chiara, P., Gaill, C. C. and Naldi, M., 1998, A Combined Geophysical Survey for Hydrogeological Purposes in North-Eastern Italy. Proceedings of IV Meeting Environmental and Engineering Geophysical Society, pp. 209 - 212.

Greenhouse J. P., DeVos, K.J., and. Pehme, P., 1997, Ground geophysical surveys for mine wastes. In Proceedings of Exploration '97, Fourth Decennial International Conference on Mineral Exploration, ed. A.G. Gubbins, 917-26. Toronto: Prospectors and Developers Association of Canada.

Guptasarma, D. and Singh, B., 1997, New digital linear filters for Hankel $J_o$ and $J_1$ transforms. Geophysical Prospecting, 45, 745-762.

Hall, D. W. and Pasicznyk, D. L, 1987, Application of seismic refraction and terrain conductivity methods at a ground water pollution site in North-Central New Jersey. In, First National outdoor Action Conference on Aquifer Restoration, Ground Water Monitoring and Geophysical Methods. Graves.

Hazell, J. R. T., Cratchley, C. R. and Jones, C. R. C., 1992, The hydrogeology of Crystalline Aquifers in Northern Nigeria and Geophysical Techniques used in their Exploration. In: E. P. Wight and W. G. Burgess, (eds), The Hydrogeology of Crystalline Basement Aquifers in Africa. Geological Society Special Publication, No. 66, pp. 155-182.

Hazell, J. R. T., Cratchley, C. R. and Preston, A. M., 1988, The Location of Aquifers in Crystalline Rocks and Alluvium in Northern Nigeria using Combined Electromagnetic and Resistivity Techniques. Quarterly Journal of Engineering Geology, vol. 21, pp. 159 - 175.

Heiland, C.A., 1968, "Geophysical Exploration". Ch10. Hafner Publishing Co. N.Y.

Hild, J. F., Blohm, R. J., Lahti, R. M. and Blohm, M. W., 1996, Geophysical Surveys for Groundwater Exploration in Northern Guam. Symposium on the Application of Geophysics to Engineering and Environmental Problems, pp. 331 - 341.

Hoekstra, P. and Blohm, M., 1990, Case Histories of Time Domain Electromagnetic Soundings. In: Ward, S. H. (Ed.), Geotechnical and Environmental Geophysics, vol. 2: Environmental and Groundwater, SEG Investigations in Geophysics, no. 5.

Keller, G.V., and Frischknecht, F. C., 1966, Electrical Methods in Geophysical Prospecting, Pergamon Press, Inc., Long Island City, New York.

Kerry L Hughes, Ann D Christy and Joe E Heimlich, 2005, 'Landfill Types and Liner Systems', Ohio State University Fact Sheet, pp 1.

Kirkham, D., 1964, "Hydrogeology", Handbook of Applied Hydrology. Ch. 5, Chow, V. T., Ed. McGraw Hill. N.Y.

Kjeldsen, P., Barlaz, M. A., Rooker, A. P., Baun, A., Ledin, A. and Christensen 2002, 'Present and Long-Term Composition of MSW Landfill Leachate: A Review, Critical Reviews in Environmental Science and Technology, vol. 32, no. 4, pp. 297-336.

Kjeldsen, P., Barlaz, M. A., Rooker, A. P., Baun, A., Ledin, A. and Christensen 2002, 'Present and Long-Term Composition of MSW Landfill Leachate: A Review', Critical Reviews in Environmental Science and Technology, vol. 32, no. 4, pp. 297-336.

MacFarlane, D. S., Cherry, J. A., Gillham, R. W. and Sudicky, E. A., 1983, 'Migration of contaminants in groundwater at a landfill: A case study : 1. Groundwater flow and plume delineation', Journal of Hydrology, vol. 63, no. 1-2, pp. 1-29.

Mack, T. J. and P. E. Maus., 1986, Detection of contaminant plumes in ground water of Long Island, New York, by electromagnetic terrain-conductivity surveys. USGS. Water-Resources Investigations. 86-4045. 39 pp.

Maimone, M., Keil, D., Lahti, R., and Hoekstra, P., 1989, Geophysical Surveys for Mapping Boundaries of Fresh Water and Salty Waters in southern Nassau County, Long Island, NY. In: Proc. Third Nat. Outdoor Action Conf. on Aquifer Restoration, Groundwater Monitoring and Geophysical Methods, National Water Well Association, Dublin, OH, pp. 965-977.

Markku Pirttijärvi, 2003, PhD Thesis Numerical Modeling and Inversion of Geophysical Electromagnetic Measurements Using a Thin Plate Model. Department of Geosciences, University of Oulu.

Maxey, G.B., 1964, "Hydrogeology", Handbook of Applied Hydrology. Ch.4, Chow, V. T., Ed. McGraw Hill. N.Y.

Mensah, A. and Larbi, E., 2005, "Solid waste disposal in Ghana" . Well Factsheet-Regional Annex (www.trend.wastsan.net) Accessed on 24th April, 2010

Mensah Anthony, Olufunke Cofie and Agnes Montangero, 2003, Lessons from a pilot co-composting plant in Kumasi, Ghana.

Meyboom, P., 1967, "Hydrogeology", Groundwater in Canada. Ch. 2. Brown, I.C., Ed. Geol. Surv. Canada, Econ. Geol. Rept. 24.

McNeill, J. D., 198, Electromagnetic terrain conductivity measurement at low induction numbers. Geonics Limited. Technical Note. TN-6. 1-15 pp.

McNeill, J. D., 1990, Use of electromagnetic methods for groundwater studies. In, Ward, S. H., ed. Pp. 191-218. Geotechnical and Environmental Geophysics, Society of Exploration Geophysicists, Tulsa, OK.

McNeill J. D., 1985, "EM 34-3 Measurements at Two Inter-Coil Spacings to Reduce Sensitivity to near-Surface Material", Technical Note Tn-19, Geonics Limited 1745 Meyerside Dr., Unit 8, Mississauga, Ontario, Canada L5T 1C5.

McQuown, M. S., Becker, S. R. and Miller, P. T., 1991, Subsurface characterization of a landfill using integrated geophysical techniques. In, Proceedings of the Fifth National Outdoor Action Conference on Aquifer Restoration, Ground Water Monitoring and Geophysical Methods, May 13-16, 1991. ed. Pp. 933-946. Water Well Journal Publishing Co., Las Vegas, NV.

Murray, R. J., Imray, B. C. and Mason, D., 1961,'The geology and economic resources of the Kumasi area', Geological Survey Ghana, Bulletin. 26. 1961. 31 p.

Nicholson, R. V., Cherry, J. A. and Reardon, E. J., 1983, 'Migration of contaminants in groundwater at a landfill: A case study 6. Hydrogeochemistry', Journal of Hydrology, vol. 63, no. 1-2, pp. 131-176.

Olayinka, A. and Barker, R., 1990, Borehole Siting in Crystalline Basement Areas of Nigeria with a Microprocessor Controlled Resistivity Traversing System. Groundwater, vol. 28, pp. 178-183.

Olhoeft, G. R.,1986, Direct detection of hydrocarbon and organic chemicals with ground penetrating radar and complex resistivity. In, Proc. of the NWWA/API Conf. on Petroleum Hydrocarbons and Organic Chemicals in Ground Water - Prevention, Detection and Restoration. ed. Pp. 284-305. National Water Well Association, Dublin OH, Houston, TX.

Olhoeft, G. R. and King, T. V. V., 1991, Mapping subsurface organic compounds noninvasively by their reactions with clays. In, Proc. 4th Toxic Substances Technical Meeting. ed. Pp. 1-18. Monterey, CA.

Paillet, F., Hite, L. and Carlson, M., 1999, Integrating Surface and Borehole Geophysics in Ground Water Studies - An Example Using Electromagnetic Soundings in South Florida.

Peter J. Hutchinson, Laura S. Barta, 2000, 'Geophysical Applications to Solid Waste Analysis', Proceedings of the Sixteenth International Conference on Solid Waste Technology and Management Philadelphia, PA U.S.A., December 10-13, 2000 Editors: Zandi, I.; Mersky, R.L.; Shieh W.K. Pp. 2-68 to 2-78.

Petersen, R., Hild, J., and Hoekstra, P., 1989, Geophysical Studies for the Exploration of Groundwater in the Basin and Range of Northern Nevada. Symposium on the Application of Geophysics t Environmental and Engineering Problems, pp.425.

Porsani, J. L., Filhob, W. M., Vagner, R. E., Shimelesa, F., Douradob, J. C and Moura, H.P., 2004, The use of GPR and VES in delineating a contamination plume in a landfill site: a case study in SE Brazil. J Appl Geophys 55:199–209.

Radcliffe, D.E., Brune, D.E., Drommerhausen, D.J. and Gunther, H.D., 1994, Dairy loafing areas as sources of nitrate in wells. p. 307–313. In Environmentally sound agriculture: Proc. Conf., 2nd, Orlando, FL. 20–24 July 1994. ASAE, St. Joseph, MI.

Ranjan, R.S., and T. Karthigesu., 1995, Evaluation of an electromagnetic method for detecting lateral seepage around manure storage lagoons. ASAE Pap. no. 952440. ASAE, St. Joseph, MI.

Reynolds, J.M., 1997, An Introduction to Applied and Environmental Geophysics. Pp 55 Wiley.

Roberts, N., Billa, M.E. and Furst, G.E., 1992, A phased approach to remediation of a complex site. In Proceedings of the National Ground Water Association focus conference on eastern regional groundwater issues, Columbus, OH.

Russell, G. M., 1990, Application of geophysical techniques for assessing groundwater contamination near a landfill at Stuart, Florida. In, 1990 FOCUS Conference on Eastern Regional Groundwater Issues. ed. Pp. 211-225. NWWA, Springfield, Mass.

Saunders, W. R. and Cox, S. A., 1987, Use of an electromagnetic Induction technique in subsurface hydrocarbon investigations. In, First National outdoor Action Conference on Aquifer Restoration, Groundwater Monitoring and Geophysical Methods. Graves. Pp. 585-601. National Water Well Association, Las Vegas, Nevada.

Sawaittayothin, V. and Polprasert, C., 2007, 'Nitrogen mass balance and microbial analysis of constructed wetlands treating municipal landfill leachate', Bioresource Technology, vol. 98, no. 3, pp. 565-570.

Scaife, J. E., 1990, Using geophysical techniques in environmental site assessments. Municipal and Industrial Water & Pollution Control. CXXVIII (4): 4-5.

Siegrist, R.L., and Hargett, D.L., 1989, Application of surface geophysics for location of buried hazardous waste. Water Manage. Res. 7:325–335.

Smedley, P.L., Edmunds, W.M. and Pelig-Ba, K.P., 1994, Mobility of Trace Elements (As, I, F) in Groundwater from Ghana and their Impact on Health. Western Africa Water and Environment Conference, May 1994 Accra Ghana.

Stenson, R. W., 1988, Electromagnetic data acquisition techniques for landfill investigations. In, Symposium on the Application of Geophysics to Engineering Problems. ed. Pp. 735-746. The Society of Engineering and Mineral Exploration Geophysics, Golden, CO.

Stierman, D.L. and Ruedisili, L.C., 1988, Integrating geophysical and hydrogeological data: An efficient approach to remedial investigations of contaminated ground water. p. 43–57. In A.G. Collins and A.J. Johnson (ed.) Ground water contamination field methods. ASTM STP 963. Am. Soc. for Testing Matl., Philadelphia.

Taylor, K., Widmer. M. and Chesley, M., 1992, Use of Time-domain Electromagnetics to Define Local Hydrogeology in an Arid Alluvial Environment. Geophysics, vol. 57, pp. 343- 352.

Todd, D.K., 1964, "Groundwater", Handbook of Applied Hydrology. Ch 13 Chow, V.T. Ed. McGraw Hill, N.Y.

Trenholm, N.M. and Bentley, L. R., 1998, The Use of Ground- Penetrating Radar to Accurately Determine Water Table Depths. Symposium on the Application of Geophysics to Environmental and Engineering Problems, pp. 829-838.

U.S. Environmental Protection Agency (EPA) '2011 Edition of the Drinking Water Standards and Health Advisories' EPA 820-R-11-002 Office of Water U.S. Environmental Protection Agency Washington, DC

Van Overmeeren R. A., 1989, Aquifer boundaries explored by geoelectrical measurements in the coastal plain of Yemen: a case of equivalence. Geophysics 54, no.1, pp. 38 – 48.

Veil Men A, K., Noye, M. and Danuor, S. K., 2005, "Prospecting For Groundwater Using The Electromagnetic Method in The Voltain Sedimentary Basin in The Northern Region of Ghana – A Case Study of The Gusihegu-Karaga District", Journal of Science and Technology , voll 25 No. 2.

Walther, E. G., Pitchford, A. M. and Olhoeft, G. R., 1986, A strategy for detecting subsurface organic contaminants. In, Proc. on Petroleum Hydrocarbons and Organic Chemicals in Groundwater - Prevention, Detection and Restoration. ed. Pp. 357-381. National Water Well Association, Houston, TX.

Wilhelm Struckmeier, Yoram Rubin and Jones, J. A. A., 2005, "Groundwater-reservoir for a thirsty planet", Earth Sciences for Society, pp 1.

World Health Organisation (WHO), 2006, Guidelines for drinking-water quality, WHO press, Geneva.

Wurmstich, B. and Morgan, F. D., 1994, Similarities in modeling groundwater flow and DC resistivity: Annual Meeting Abstracts, Society of Exploration Geophysicists, 578 - 579.

Yang, C., Tong, L. and Jeng, L., 1994, Locating groundwater at selected sites by geoelectric methods: Annual Meeting Abstracts, Society of Exploration Geophysicists, 652-654.

Yang, C. and Lee, W., 1998, Using resistivity sounding and geostatistics to aid in hydrogeological studies in the Choshuichi alluvial fan, Taiwan: Annual Meeting Abstracts, Society of Exploration Geophysicists, 832 - 835.

Young, M. E., de Bruijn, R. G. M. and Al- Ismaily, A. S., 1998, Exploration of an Alluvial Aquifer in Oman by time - domain Electromagnetic Sounding. Hydrogeology Journal v6., pp. 383-393.

## APPENDIX

### Theory of Operation at Low Induction Numbers

There are two types of coil configuration as shown in figure A1 below

a. Vertical dipole
b. Horizontal dipole

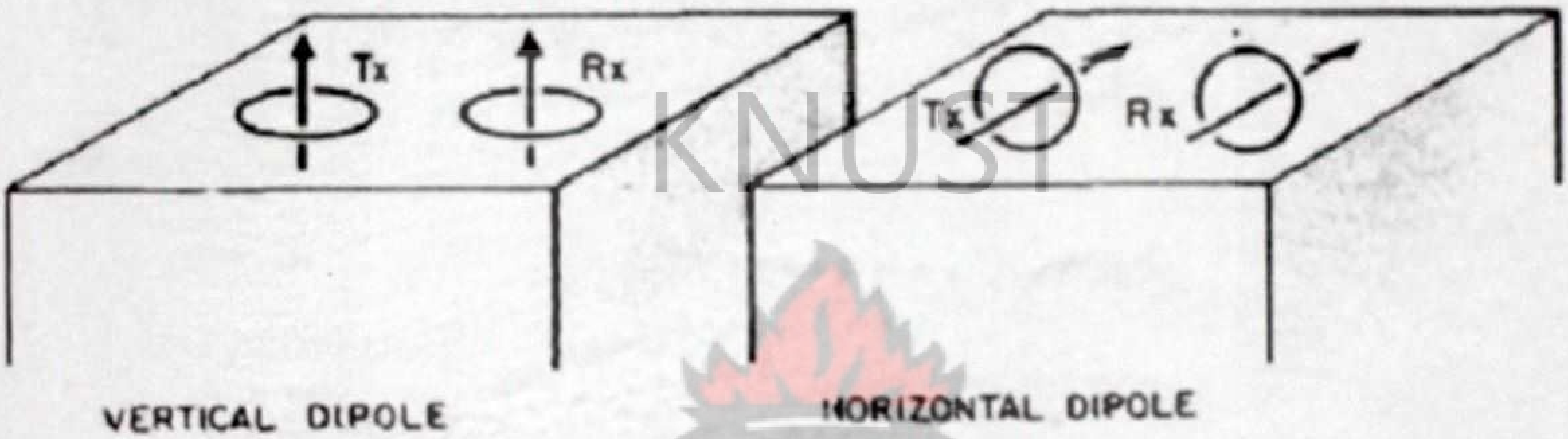


**Figure A1 Vertical and Horizontal Dipole configuration**

The Transmitter coil ($T_x$) is energized with alternating current at a frequency of f Hertz. For the EM34-3 instrument the frequency of the alternating current is fixed for each coil separation, *s* in meters

Table A 1 coil separation and corresponding frequency

| **Coil Separation (s) M** | **Frequency kHz** |
|---|---|
| 10 | 6.4 |
| 20 | 1.6 |
| 40 | 0.4 |

The receiver ($R_x$) measures the ratio of the Secondary magnetic field $H_S$ to the primary magnetic field $H_P$ ($\frac{H_S}{H_P}$).

A complicated function of the variable $\gamma s$ which is in turn a complex function of frequency and conductivity define the field ratios of the vertical and horizontal dipole configuration as given in equation (1) and (2) below.

$$\left(\frac{H_s}{H_p}\right)_V = \frac{2}{(\gamma s)^2}\{9 - [9 + 9\gamma s + 4(\gamma s)^2 + (\gamma s)^3]e^{-\gamma s}\} \quad \text{(A1)}$$

$$\left(\frac{H_s}{H_p}\right)_H = 2\left[1 - \frac{3}{(\gamma s)^2} + [3 + 3\gamma s + (\gamma s)^2]\frac{e^{-\gamma s}}{(\gamma s)^2}\right] \quad \text{(A2)}$$

Where $\gamma = \sqrt{i\omega\mu_o\sigma}$

$\omega = 2\pi f$

$f = frequency\ (Hz)$

$\mu_o = permeability\ of\ free\ space$

$i = \sqrt{-1}$

A well-known characteristics of homogeneous half-space is the electrical skin depth $\delta$ which is define as the distance in the half-space that a propagating plane wave has travelled when its amplitude has been attenuated by 1/e of the amplitude at the surface. The expression for the skin depth is given in equation (A3) below

$$\delta = \sqrt{\frac{2}{\omega\mu_o\sigma}} = \frac{\sqrt{2i}}{\gamma} \quad \text{(A3)}$$

and therefore

$$\gamma s = \sqrt{2i}\frac{s}{\delta} \quad \text{(A4)}$$

Induction number $B$ is equal to the ratio of the intercoil spacing divided by the skin depth $\delta$

$$B = \frac{s}{\delta}$$

$$\gamma s = \sqrt{2i}\, B \tag{A5}$$

Now if $B$ is much less than unity (i.e. $\gamma s \ll 1$) the field ratios of equation (A1) and (A2) reduces to

$$\left(\frac{H_s}{H_p}\right)_V \cong \left(\frac{H_s}{H_p}\right)_H \cong \frac{(\gamma s)^2}{4} = \frac{iB^2}{2} = \frac{i\omega\mu_o\sigma s^2}{4} \tag{A6}$$

The magnitude of the secondary magnetic field is now directly proportional to the ground conductivity and the phase of the secondary magnetic field leads the primary magnetic field by $90^0$.

To make $B$ much less than unity we see that we must make $s$ very much less than $\delta$ and thus

$$\omega \ll \frac{2}{\mu_o\sigma s^2} \tag{A7}$$

That is, having decided on a value for $s$ (which fixes the effective depth of penetration under the condition $B \ll 1$), the maximum probable ground conductivity is estimated and the operating frequency is chosen so that equation (A7) is always satisfied. The apparent conductivity which the instrument reads is then defined by

$$\sigma_a = \frac{4}{\omega\mu_o s^2}\left(\frac{H_s}{H_p}\right)_{quadrature\ component} \tag{A8}$$

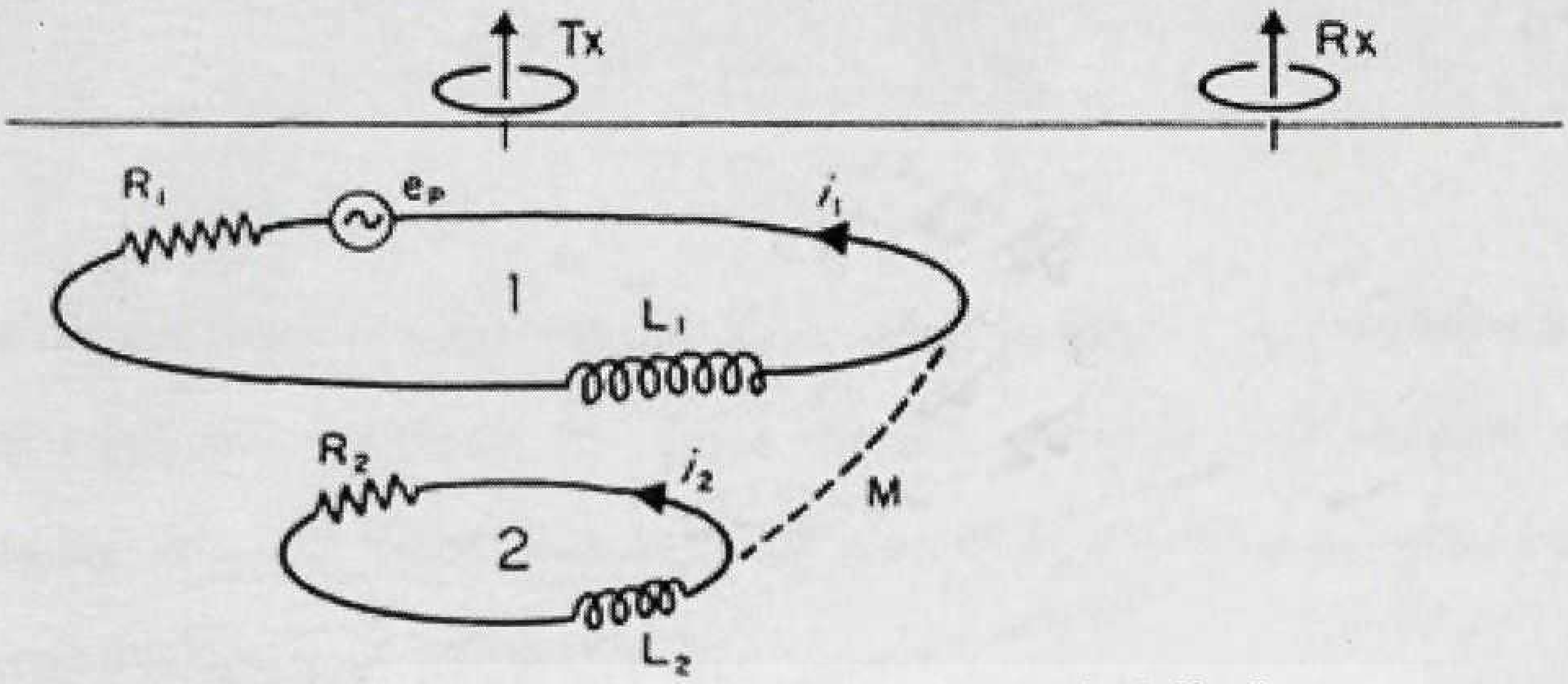


**Figure A2 Electrical model for vertical dipoles**



Equation (A8) above can be explained by examining the vertical dipole configuration shown in Figure A2 above.

Let's consider current loop 1. Through Faraday's law the primary emf $e_p$ causing this current to flow is given by the time rate of change of the primary magnetic flux from the transmitter through the loop. The current through the loop is limited by three impedances given below,

(i) The electrical resistance $R_1$ of the loop
(ii) The self-inductance $L_1$ through the loop
(iii) The mutual-inductance, $M$ coursed by caused by magnetic fields in other current loops such as $i_2$.

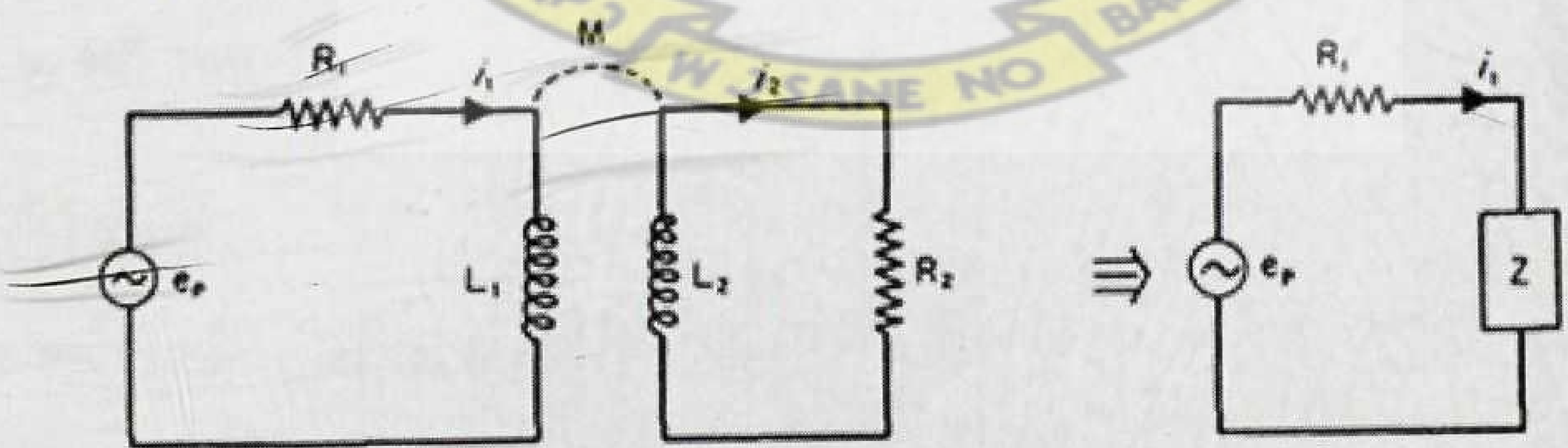


Figure A3 Equivalent circuit for model of figure A.2

The equivalent circuit for this configuration is easily derived from elementary circuit theory with the result shown in Figure A.3

$$Z = i\omega L_1 + \frac{\omega^2 M^2}{R_2 + i\omega L_2}$$

$$i_1 = \frac{e_P}{R_1 + Z}$$

The complex impedance Z incorporates all the effects of magnetic coupling between current loop 1 and any other current loop 2. The impedance Z can be made arbitrarily small by reducing $\omega = 2\pi f$, the operating frequency. When Z is thus made much smaller than $R_1$ the current flow in loop 1 is simply given by

$$i_1 = \frac{e_P}{R_1} = \frac{i\omega \emptyset_P}{R_1} = i\omega \emptyset_P G_1 \qquad \text{(A9)}$$



Where $\emptyset_P$ = primary flux linking loop 1

$G_1$= conductance of loop 1 $(G_1 = 1/R_1)$

$$i = \sqrt{-1}$$

We see from equation (A9) above that the magnitude of the current is linearly proportional to the loop conductance and furthermore that the phase of the current leads the primary flux by $90^0$. Since the secondary magnetic field at the receiver from current $i_1$ is in phase with and directly proportional to $i_1$ it too will be directly proportional to G and will lead the primary flux by $90^0$. Thus

$$\left(\frac{H_s}{H_P}\right) \propto i\omega G_1 \qquad \text{(A10)}$$

This has the same dependence on frequency and conductance as equation (A6). It can infer therefore, that the condition $B \ll 1$ is equivalent to stating that for all current loops that affect the receiver output the operating frequency is so low that we can ignore any magnetic coupling between the loops. Thus the current that flows in any loop is (i) completely independent of the current that flows in any other loop since they are not magnetically coupled and (ii) is only a function of the primary magnetic flux linking that loop and of the local ground conductivity

The lack of interaction between current loops is of great importance in simplifying the data reduction procedures. It is proof the fact that for any value of induction number B and for any orientation of a magnetic dipole over a uniform halfspace or horizontally stratified earth the current flow is horizontal. Thus, in a horizontally layered earth no current crosses an interface.



If no current flow crosses an interface and if there is no magnetic coupling between current loops, changing the conductivity of any one of the layers of a horizontally stratified earth will not alter the geometry of the current flow. Varying the conductivity of any layer will proportionately vary only the magnitude of the current in that layer. To calculate the resultant magnetic field at the surface of a horizontally layered earth it is simply necessary to calculate the independent contribution from each layer, which is a function of its depth and conductivity and to sum all contributions

$$\emptyset_V(Z) = \frac{4z}{(4Z^2+1)^{3/2}} \quad \text{(A11)}$$

$$\emptyset_H(Z) = 2 - \frac{4z}{(4Z^2+1)^{1/2}} \quad \text{(A12)}$$

$$R_V(Z) = \frac{1}{(4Z^2+1)^{1/2}} \quad \text{(A13)}$$

$$R_H(Z) = (4Z^2+1)^{1/2} - 2Z \quad \text{(A14)}$$

The functions $\emptyset(z)$ and $R(z)$ above define the relative influence of current flow as a function of depth. Where $(Z)$ is the depth divided by the intercoil spacing.

Finally it should be noted that for a given frequency and intercoil spacing as the terrain conductivity increases the approximation of the equation (A6) eventually breaks down and the instrumental output is no longer proportional to terrain conductivity. The effect is illustrated in Figure A.2

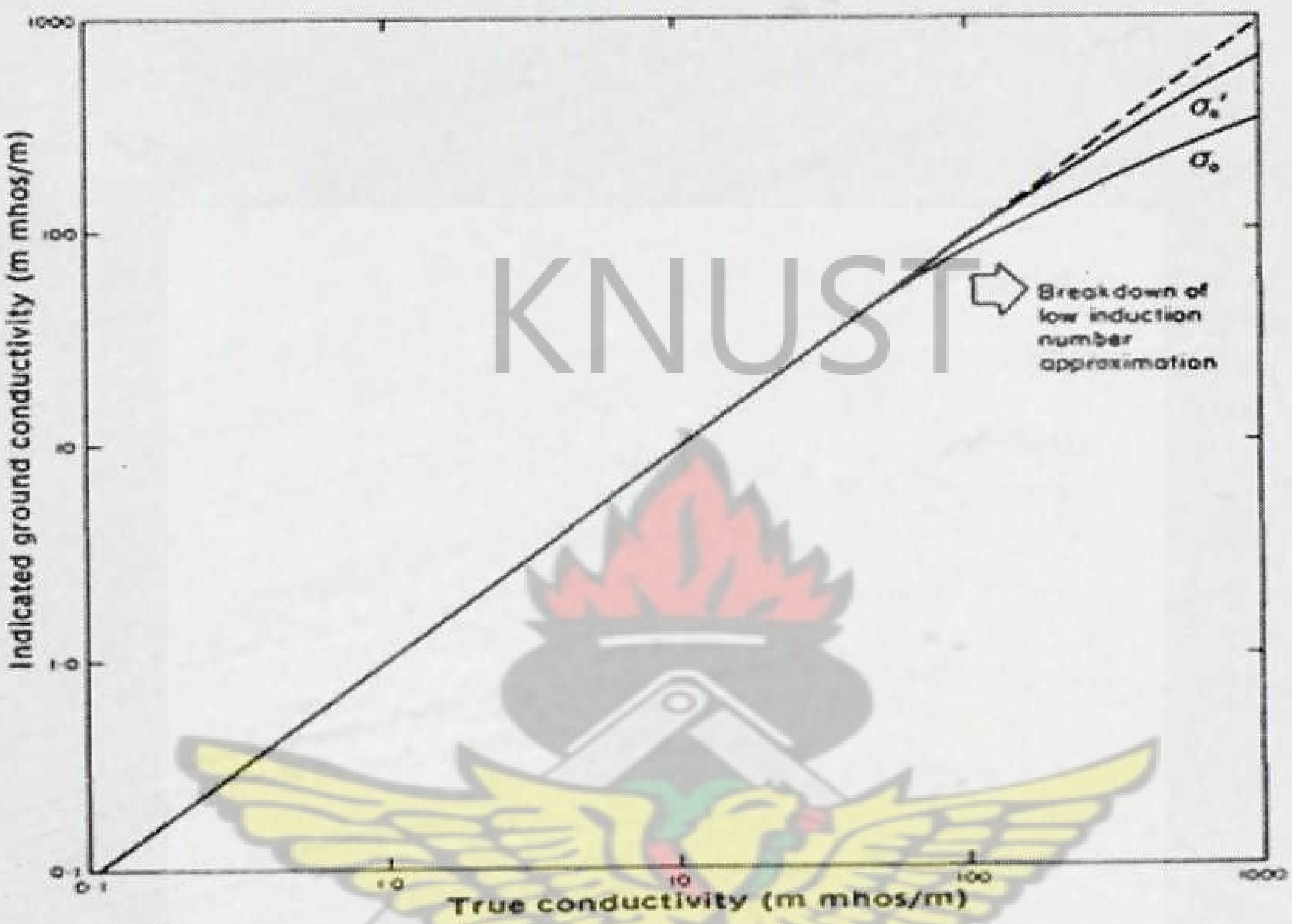


Figure A4. Plot of indicated conductivity for EM31 versus true conductivity for both vertical ($\sigma_a$) and horizontal ($\sigma'_a$) dipoles